ZOOLOGICAL SCIENCE 17: 911–933 (2000)

Morphological Characteristics of the Developing Cranial Nerves and Mesodermal Head Cavities in Sturgeon Embryos from Early Pharyngula to Late Larval Stages

Shigeru Kuratani*, Yoshiaki Nobusada, Hajime Saito and Yasuyo Shigetani

Department of Biology, Faculty of Science, Okayama University 3-1-1 Tsushimanaka, Okayama 700-8530, Japan

ABSTRACT—As sturgeons are considered to represent a basal group of Osteichthyes, it is necessary to evaluate their developmental features to understand the evolution, not only of bony fishes, but also of tetrapods in general. Using Besters, commercially established hybrid sturgeons, the neural crest cell distribution pattern, mesodermal epithelium, and peripheral nerves were observed based on whole-mount immunostained and -sectioned embryos, from the pre-hatching embryonic stage to a late swimming larval stage. At the early pharyngula stage, the hindbrain exhibits at least six rhombomeres. These have a typical arrangement of neuroepithelial cells, and segmentally distributed cephalic crest cell populations associated with even-numbered rhombomeres medially, and single pharyngeal arches laterally. The head cavities first arise as a pair of epithelial primordia in the prechordal region. Secondarily, the cavity is subdivided mediolaterally into the premandibular and mandibular cavities. These mesodermal components never affect the segmental pattern of cranial nerve roots as seen in the shark embryo (Kuratani and Horigome, 2000), probably due to the early degeneration of the cavities. The hyoid cavity never appears. As observed in several teleosts, the newly hatched Bester larva possesses extensive neurites in the epidermis, originating from both trigeminal placodes and Rohon-Beard cells. This neurite network diminishes during development, in concordance with the appearance of lateral line nerves. All the epibranchial placodes are seen as focal, HNK-1-positive epidermal thickenings and give rise to inferior ganglia of the branchiomeric nerves. Metameric morphology of the branchiomeric nerve innervation is secondarily disturbed through modification of the head region, involving the expansion of the operculum and modification of the jaw.

INTRODUCTION

Sturgeons are generally regarded as one of the most primitive groups among Osteichthyes since a large part of their endoskeleton remains cartilaginous and several anatomical features resemble those of sharks. However, their Paleozoic ancestors are now known to have possessed highly ossified skeletal systems. As a sister group of polypterids, sturgeons have been classified in Chondrostei until recently. They are now considered to belong to the group Acipenseriformes, together with paddle fish, gars, and *Amia* (bowfin) (Grande and Bemis, 1996), although their phylogenetic position still remains enigmatic (see Bond, 1996; and references therein). Nevertheless, sturgeons and those fish that belong to the Holostei (gars and *Amia*; Romer and Parsons, 1977) possess a number of features that are absent from teleosts. Along with the uneven holoblastic cleavage, not discoidal as in teleosts, the embryos exhibit an expanded head region over the yolk at early pharyngular stage, reminiscent of amphibian development (Balfour and Parker, 1882; Dean, 1895; Eycleshymer and Wilson, 1906). Their early larvae also resemble those of amphibians (Kerr, 1900, 1901; reviewed by Keibel, 1906). Lungfish share these apparently primitive features. Acipenseriformes and teleosts also share a similar mode of gastrulation (Keibel, 1906). Sturgeons thus represent an important group of animals in the understanding of the embryogenetic changes that took place in the evolution of Osteichthyes as well as of tetrapods.

Except for the developmental stages (Bolker, 1993), the embryonic development of sturgeons has been less extensively studied than for Chondrichthyes. In the latter group, pharyngula embryos were previously believed to exhibit a typical vertebrate body plan. This judgment was based on the possession of head cavities (segmented head mesoderm), and well-segmented peripheral nerve primordia, including neural crest cell populations and epibranchial placodes that are associated with the metameric pattern of pharyngeal arches (Balfour, 1878; van Wijhe, 1882; Kupffer, 1891; Goodrich, 1930; Batten, 1957a, b; Bjerring, 1977; reviewed

* Corresponding author: Tel. +81-86-251-7867;
FAX. +81-86-251-7876.
E-mail. sasuke@cc.okayama-u.ac.jp

by Jarvik, 1980). In particular, the presence of segmented mesoderm, or head cavities, was previously compared with the segmentation of somites in the trunk, and these epithelial mesodermal regions maintain a close relationship with peripheral nerve distribution in the shark embryo (Kuratani and Horigome, 2000). The head cavities become less distinct in amniotes, although epithelial mesodermal cysts do develop in many species at late stages of pharyngula. Instead, amniotes exhibit incomplete segmentation in head mesoderm that does not seem to have any relationship with peripheral nerve patterning (reviewed by Kuratani, 1997). Thus, the evolutionary transition of mesodermal development remains unclear. Although primitive bony fish, including sturgeons, also exhibit head cavities (Ostroumow, 1906; de Beer, 1924; reviewed by Brachet, 1935; and by Jacob *et al.*, 1984), their developmental sequence and topographical relationships have not been reported.

The problem of vertebrate head segmentation is becoming a serious topic of developmental biology, in which cellular and molecular aspects of morphogenesis are analyzed. Compartmentalized segments are present in the developing brain as neuromeres, being established through restriction of neuroepithelial cell lineages (Fraser *et al.*, 1990), and segmentally regulated gene expression. These features are also shared by neural crest cell populations and the mesenchyme derived from the neurectoderm, clearly showing the presence of a metameric developmental program in the head of vertebrate embryos (Lumsden and Keynes, 1989; Figdor and Stern, 1993; reviewed by Kuratani, 1997; and by Kuratani *et al.*, 1999). Among such developmental compartments, rhombomeres are the segments in the hindbrain, and two successive segments correspond to a single pharyngeal arch by means of branchiomeric nerves (reviewed by Lumsden and Keynes, 1989).

It is necessary to evaluate the embryonic morphology of Osteichthyes, not only to understand the vertebrate body plan, but also to trace the changes of morphogenetic processes in evolution. For that purpose, sturgeons are very suitable for comparative and evolutionary studies. Here, we used the Bester, a commercially established hybrid between *Acipenser ruthenus* and *Huso huso* (beluga), maintained artificially fertilized eggs, and obtained a series of developing embryos. Based on histological and whole-mount specimens, we found that the rhombomeres and cranial nerve morphology of the Bester are well conserved, but that the developmental sequence of the head mesoderm is apparently modified as compared with other vertebrates.

MATERIALS AND METHODS

Whole-mount immunostaining

Fertilized Bester eggs (a gift from Tsukuba Research Institute, Fujikin Inc. Ltd., Tsukuba, Japan) were brought into the laboratory and kept in fresh water at 16–17°C. Embryonic stages were determined according to body length and morphological features that were consistent with the post-oviposition age (Table 1). To observe the peripheral nerve morphology in developing Bester embryos and larvae, we tested several different monoclonal antibodies that had been shown to recognize neurons. Of these, HNK-1 (Leu-7, Becton Dickinson, San Jose, CA) was the most suitable for this purpose. To obtain stability of the carbohydrate epitope as well as permeability of the antibody, embryos and larvae were fixed with Bouin's fixative at 4°C for 1 day. The embryos were washed and dehydrated in a graded series of ethanol (70%, 95%) and stored at 4°C. They were placed in Dent's fixative, a mixture of dimethyl sulfoxide (DMSO) and methanol (1:4) for several days for de-pigmentation and blocking of endogenous peroxidase activities. Half a ml of 10% Triton X-100/distilled water was added and the embryos were further incubated for 30 min at room temperature. After washing in Tris-HCl-buffered saline[OLE4] (TST: 20 mM Tris-HCl, pH 8.0, 150 mM NaCl, 0.01% Triton X-100), the samples were blocked with 5% non-fat dried milk in TST (TSTM). The embryos were incubated in the primary antibody (HNK-1, diluted 1/100 in spin-clarified TSTM containing 0.1% sodium azide) for 2 to 4 days at room temperature while being gently agitated on a shaking platform. The secondary antibody used was horseradish peroxidase (HRP)-conjugated goat anti-mouse IgM (ZYMED Lab. Inc., San Francisco, CA) diluted 1/200 in TSTM. After final washing in TST, the embryos were preincubated with peroxidase substrates 3,3'-diaminobenzidine (DAB: 100 μg/ml) in TS for 1 hr. They were allowed to react in Tris-HCl-buffered saline at the same concentration of DAB with 0.01% (v/v) hydrogen peroxide (35% aqueous solution) for 20 to 40 min at 0°C. The reaction was stopped, and the embryos were placed in 0.5% KOH. The latter treatment successfully cleared the soft tissue of the embryos (Fig. 1). The stained embryos were then transferred to a graded series of glycerol/water solutions, and stored in 60% glycerol in water for observation.

Table 1. Developmental stages of bester

specimen	body length (mm)	post-oviposition age (days)	stages
404N2	–	2	x
40424P	–	2.5	y
4056P	–	3	z
418	–	3	A
418–1140	–	3	A
419–1235	6.5	4	B
420–1330	9.0	5	C
421–1200	10.0	6	D
421–2145	11.0	6	D
422–2210	11.0	7	E
423	11.0	8	E
425–2300	14.5	10	F
429–1420	19.5	14	G

For staining of the muscle tissue, MF-20 antibody (purchased from the Developmental Studies Hybridoma Bank, Iowa City, Iowa) was used for the primary antibody. In this case, embryos were fixed with 4% paraformaldehyde in 0.1% phosphate-buffered saline at 4°C for 1 day.

Immunostaining of sectioned specimens

Specimens fixed with Bouin's fixative were embedded in paraffin and sectioned at 7 μm. They were deparaffinized and treated with 1% periodic acid for 5 min at room temperature, followed by washing in TST. The monoclonal antibody, HNK-1, was used to label the developing nervous system on the sectioned specimens. The primary antibody were diluted in TSTM and applied to the sections for 1.5 hr at room temperature. After washing with TST, secondary antibodies, HRP-anti mouse IgM (ZYMED Lab. Inc.), were diluted 1/200 in TSTM and applied to the specimens for 40 min. The sections were counter-

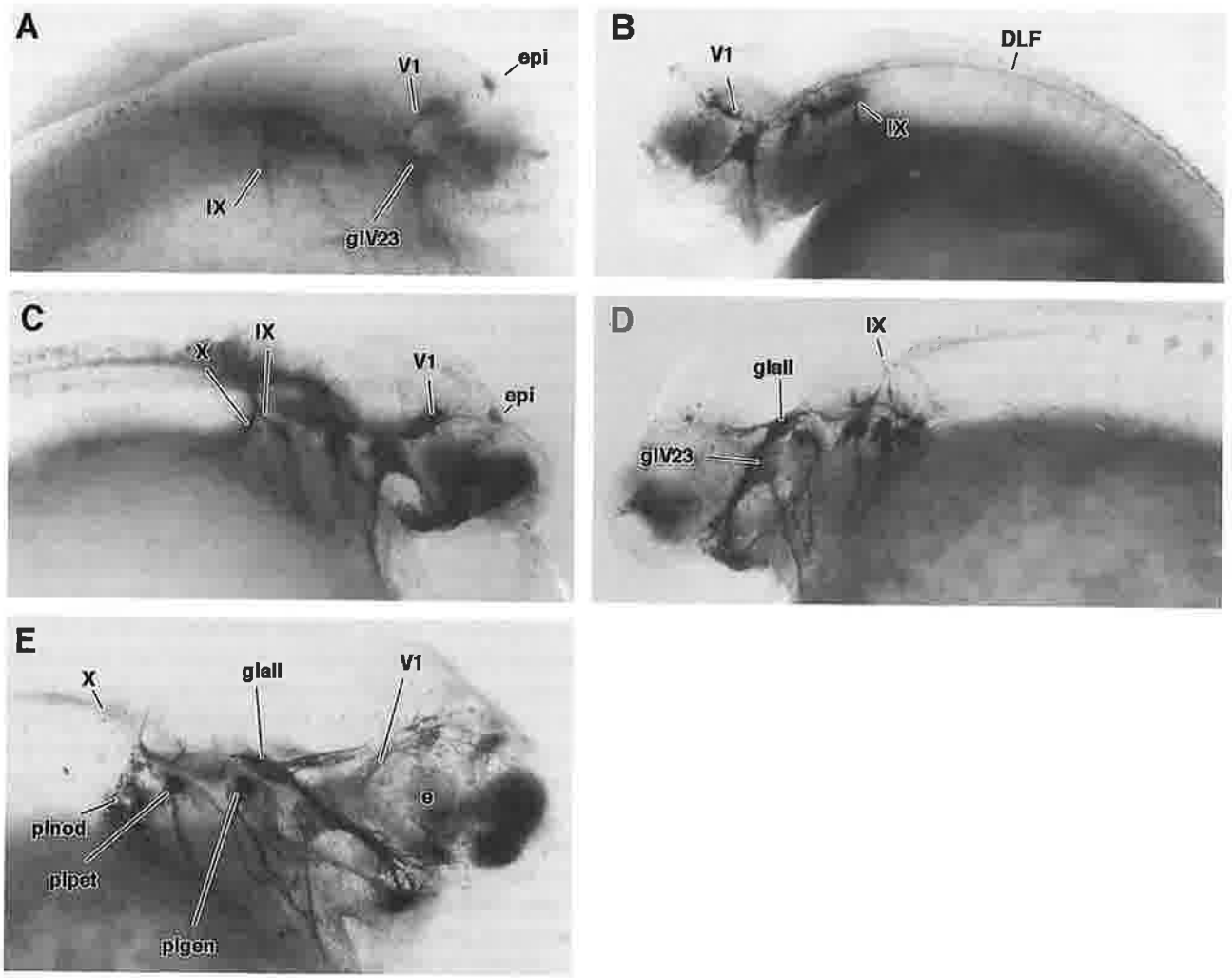

Fig. 1. Whole-mount Bester embryos and larvae immunochemically stained with HNK-1 antibody and treated with 0.5% KOH. Lateral views. Stages A (A) to E (E) are shown. For similarly treated embryos at stage F, see Fig. 10C. Only part of the neural structures are labeled. For detailed descriptions and scales, see the following line drawings.

stained either with cresyl violet or hematoxylin after the peroxidase reaction.

Abbreviations

ac	anterior commissure
all	anterior lateral line nerve
ao1	aortic arch 1
ba	barbel or its primordium
BC	branchial crest cells
com	communicating branch of the lateral nerves
cp	posterior commissure
da	dorsal aorta
di	diencephalon
dlf	dorsolateral fasciculus
drg	dorsal root ganglion
e	eye
epi	epiphysis
exg	external gills
exn	external nares
fb	forebrain
fp	frontal process (=Haftorgan of von Kupffer, 1906)
glgn	geniculate ganglion of the facial nerve
glall	anterior lateral line nerve ganglion
glmid	middle lateral line nerve ganglion
glpll	posterior lateral line nerve ganglion
glpt	petrosal ganglion of the glossopharyngeal nerve
gV23	trigeminal ganglion
h	heart
hb	hindbrain
hc	head cavity
HC	hyoid crest cells
hm	hyomandibular ramus of the facial nerve
hyc	hyoid cavity of the shark embryo
hyp	hypophysis
hypt	hypothalamus
II	optic nerve
III	oculomotor nerve
IV	trochlear nerve
IX	glossopharyngeal nerve or its anlage
mb	midbrain
mid	middle lateral line nerve
mlf	medial longitudinal fasciculus
mm	mandibular arch muscle plate
mmp	maxillomandibular prominence
mn	mandibular process
mnd	mandibular mesoderm in the lamprey

mnc	mandibular cavity
mx	maxillary process
myo	myotomes
nolf	olfactory nerve
nt	notochord
olep	olfactory epithelium
op	operculum
opm	oropharyngeal membrane
ot	otocyst
ov	optic vesicle
pa2–3	pharyngeal arches 2 to 3
pf	pectoral fin
phr	pharynx
plgen	geniculate placode
plnod	nodose placode
ploph	ophthalmic placode
plpet	petrosal placode
pltrg	trigeminal placode
poc	postoptic commissure
pog	preoral gut
pp1–3	pharyngeal pouches 1 to 3
prc	pericardium
prcm	prechordal mesenchyme
prmc	premandibular cavity
prnd	pronephric duct
r1–6	rhombomeres 1 to 6
rb	buccal branch of the anterior lateral line nerve
RB	Rohon-Beard cells
rop	opercular ramus of the facial nerve
rophs	superficial ophthalmic branch of the anterior lateral line nerve
rpd	dorsal pharyngeal branch of the glossopharyngeal nerve
rpl	palatine branch of the facial nerve
rpll	posterior branch of the posterior lateral line nerve
rprIX	pretrematic branch of the glossopharyngeal nerve
rptIX	posttrematic branch of the glossopharyngeal nerve
rptVII	posttrematic branch of the facial nerve
rptX1	posttrematic branch of n. X1
rr	rostral (or maxillary) branch of the trigeminal nerve
rv	ventral (or mandibular) branch of the trigeminal nerve
soc	tract of supraoptic commissure
som	somites
spt	supratemporal branch of the posterior lateral line nerve
tel	telencephalon
thc	tract of habenular commissure
tpoc	tract of postoptic commissure
V	trigeminal nerve or its primordium
V1	profundal nerve or its primordium
V23	trigeminal nerve
v4	fourth ventricle
VII	facial nerve
VIII	acoustic nerve
X	vagus nerve

RESULTS

Stage A

The youngest Bester embryo observed in the present study corresponded to an early pharyngula (Fig. 2). The brain at this stage resembled that seen in 70-hr embryos of *Acipenser sturio* by von Kupffer (1906; Fig. 3A). The processus neuroporicus protruded at the site of the closure of the neural pore, and a parencephalic prominence (von Kupffer, 1906), or saccus dorsalis (Nieuwenhuys, 1997), were recognized in front of the epiphysis (Fig. 3A). The epiphysis was strongly immunoreactive to HNK-1, and was associated with a nerve tract, the tract of habenular commissure, which was also HNK-1-positive (Fig. 3A, 4C, also see Figs. 6 and 8 in later stages). The telencephalon was not clearly distinguished from the rest of the forebrain. The anterior tip of the notochord had already emerged at a level slightly caudal to the plica encephali ventralis (Figs. 2B, 3A).

Putative crest cell populations were attached to discrete positions on the dorsolateral aspect of the hindbrain (Fig. 4A). Although rhombomeres were not clearly seen on the surface of the hindbrain, the arrangement of the neuroepithelial cells showed typical neuromeric morphology. In the middle of each rhombomere, neuroepithelial cells were arranged in a fan-shaped pattern and their nuclei located more basally within the epithelium than those in the boundary region (Fig. 3A). Segmental boundaries of rhombomeres were thus identified and the second and third crest cell populations were found associated with rhombomere 4 (r4) and r6, respectively.

The most rostral crest cells had mostly differentiated into the trigeminal nerve anlage containing HNK-1-positive neurons (Fig. 4C). The trigeminal ganglion and (presumably) sensory ganglia of other branchiomeric nerves seemed to contain crest-derived neurons. The trigeminal ganglion grew two branches: a rostral branch that sent fine rami covering the forebrain and optic regions, and a ventral branch that grew and ramified ventrally into the wall covering the yolk sac, beyond the future mandibular arch (Fig. 3B, see below). These branches corresponded to maxillary and mandibular branches of later stages (see below). The trigeminal nerve grew from putative r2, the most expanded region of the hindbrain.

All the embryos at this stage possessed the profundal nerve and ganglion in the cavum epiptericum (the space ventrolateral to the plica encephali ventralis), similar to other Osteichthyes embryos and larvae (Landacre, 1912). Although the position of the ganglion in the cavum appears to be a peculiar one, a similar topography has been illustrated in the earliest profundal nerve anlage of several vertebrates, including amniotes (Stone, 1922; Adelmann, 1925; Kuratani and Tanaka, 1990). Equivalent nerves of the lamprey and shark do not show such topography (Goette, 1914; Kuratani *et al.*, 1997; Kuratani and Horigome, 2000). The Bester profundal ganglion at this stage was still in contact with the epidermal placode, indicating active contribution of the placode to ganglion cells (Fig. 3B, 4H; see below). Proximally, this nerve did not contact the trigeminal nerve, but had an independent root on the hindbrain rostral to the trigeminal nerve root (see below). Neurites from other cranial sensory ganglia had also grown centrally to merge into the dorsolateral fasciculus (Fig. 4C, D).

Caudal to the trigeminal nerve, acusticofacial and glossopharyngeal nerves had formed. The primordia of geniculate and petrosal ganglia contacted the focal thickenings of the surface ectoderm at the levels of the first and second pharyngeal pouches, indicating the contribution of epibranchial placodes to these ganglia (Fig. 3B). From the geniculate gan-

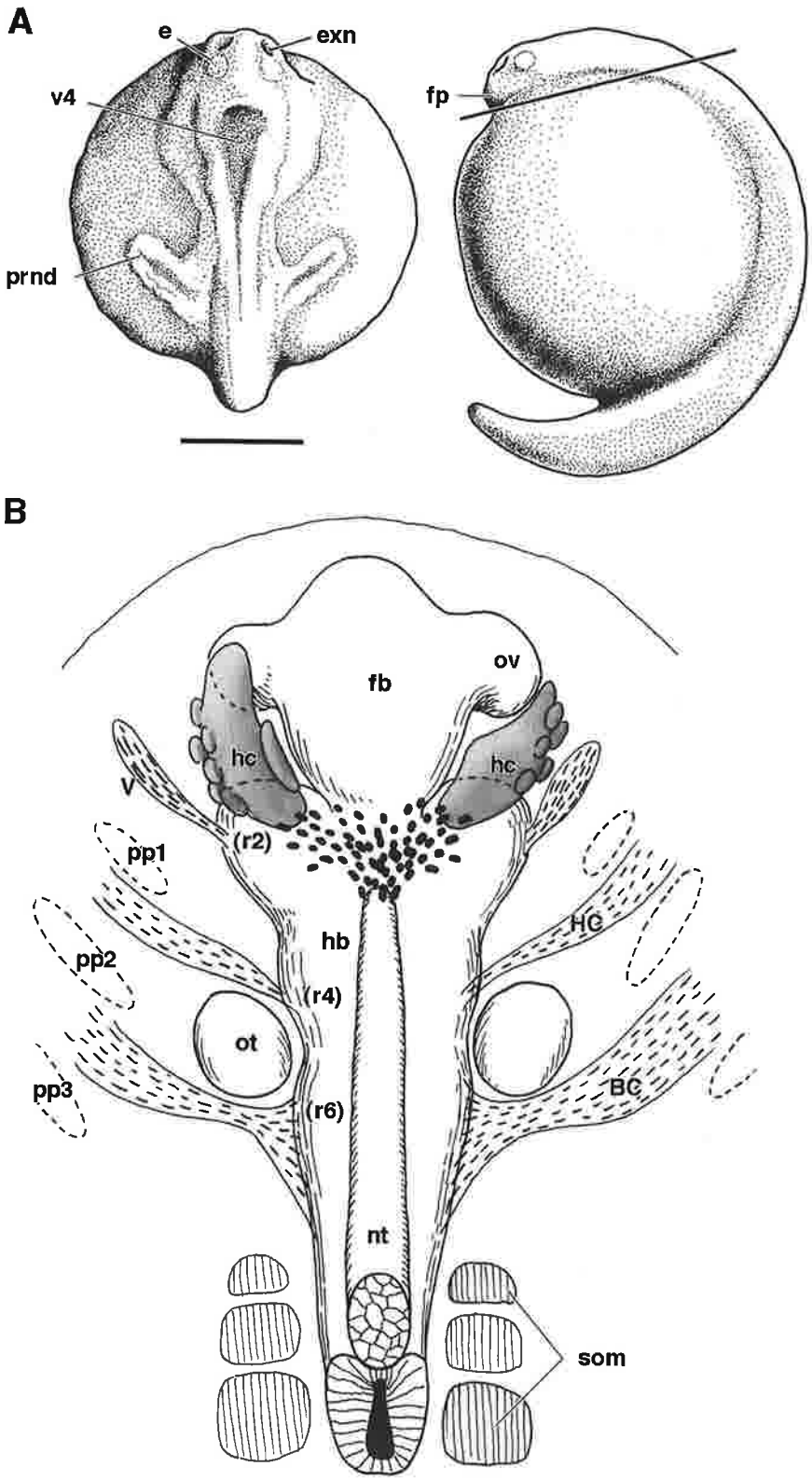

Fig. 2. Stage A embryos of Bester. **A**: External morphology of the embryo. Dorsal (left) and lateral (right) views. The line indicates the plane from which the reconstruction was viewed in B. **B**: Ventral view of the reconstructed embryo. Three cephalic crest cell populations (V, HC, BC) extend from the hindbrain and are peripherally distributed in each pharyngeal arch. Of those, the most rostral cell population has differentiated into the trigeminal nerve ganglion (V). Beneath the optic vesicle (ov), a pair of mesodermal epithelia, or head cavities (hc) has developed. The basal surface of the cavity is rough and is associated with small protrusions or independent epithelial cysts. Note that a dense mesodermal mesenchyme is present, connecting the pair of head cavities and the rostral tip of the notochord (nt). Bar = 1 mm.

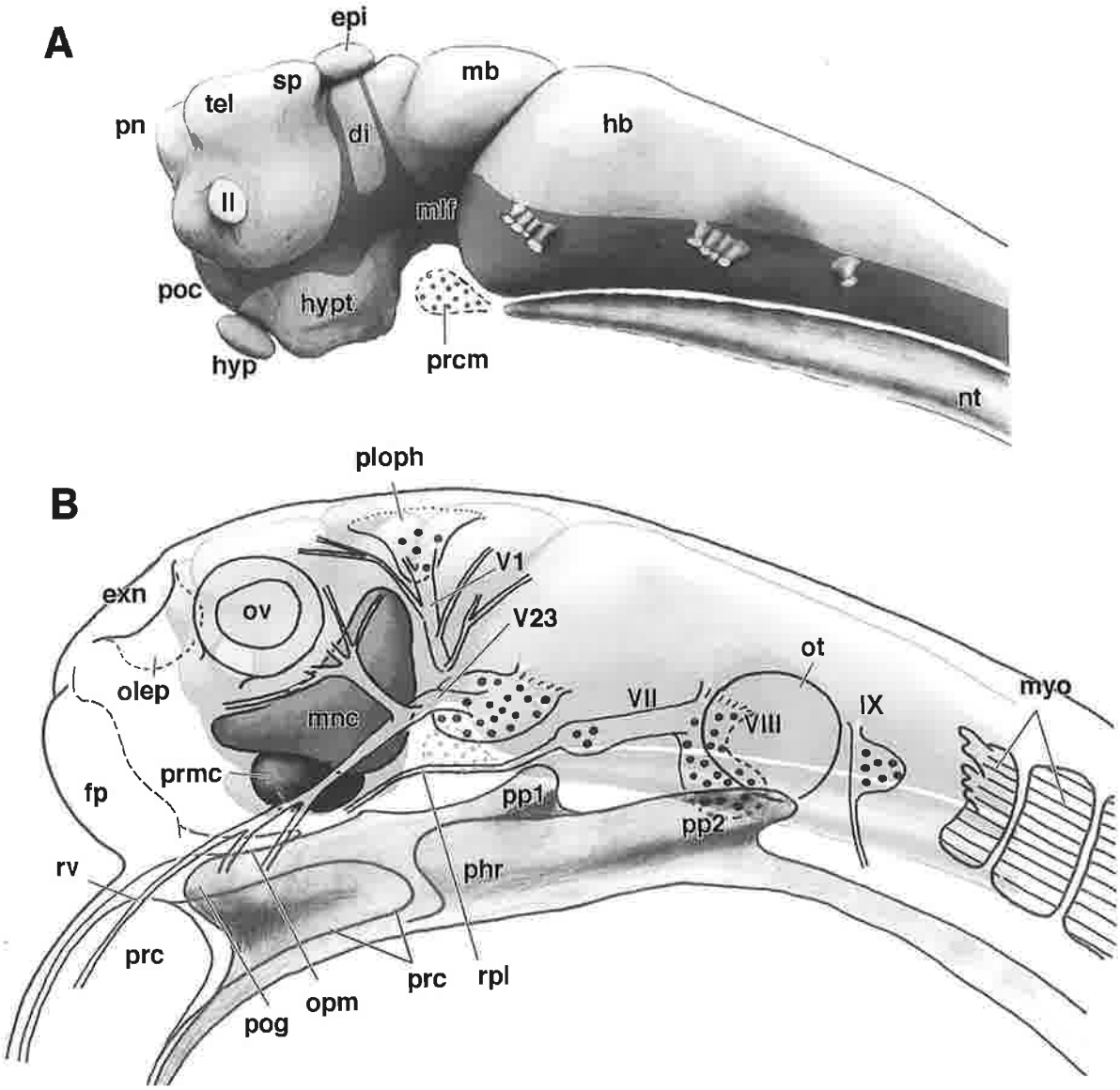

Fig. 3. Graphic reconstruction of a stage A embryo. Lateral views. **A**: External morphology of the brain. The developing nerve tracts are shaded. Note the prechordal mesenchyme (prcm) beneath the plica encephali ventralis. **B**: Reconstructed embryonic structures are superimposed on the brain. Peripheral nerve ganglia are stippled. This embryo is slightly older than that illustrated in Fig. 2B. The head cavity has been incompletely separated into two components, the medial, or the premandibular cavity (prmc), and the more laterally located mandibular cavity (mnc). Note that the mandibular cavity is inserted between profundal (V1) and trigeminal (V23) nerves.

glion, a branch grew rostrally for a long distance into the future upper jaw region, representing the palatine branch of the facial nerve that innervates barbels at later stages. All the branchiomeric nerve roots were proximally connected to the dorsolateral fasciculus. The latter tract contained fibers from the above-noted sensory ganglia and Rohon-Beard cells in the caudal part of the hindbrain and the spinal cord (Fig. 4C to E).

Rostral to the anterior tip of the notochord, beneath the cephalic flexure, was a dense mesenchyme that expanded rostrolaterally to attach to a pair of mesodermal epithelial structures, the head cavities, on both sides of the diencephalon and beneath the optic vesicle (Fig. 2B). The cavities were spindle-shaped, with a number of small cysts and epithelial processes on the surface (Fig. 2B). In slightly older embryos, the cavities began to be divided into a small and ventrally located cavity, and a dorsally located larger cavity on each side (Fig. 3B). The latter was located between the ophthalmic profundus nerve and the maxillomandibular nerve (Figs. 3B, 4H, I). From the position and morphology, this cavity corresponded to the mandibular cavity of the shark embryo (Galeus canis: van Wijhe, 1882; 4.5-mm *Squalus acanthias*: de Beer, 1922; *Scyliorhinus torazame*: Kuratani and Horigome, 2000), and the smaller one to the premandibular cavity (Kuratani and Horigome, 2000; and refs. therein). These cavities were not separated completely from each other (Fig. 4F to I). In no

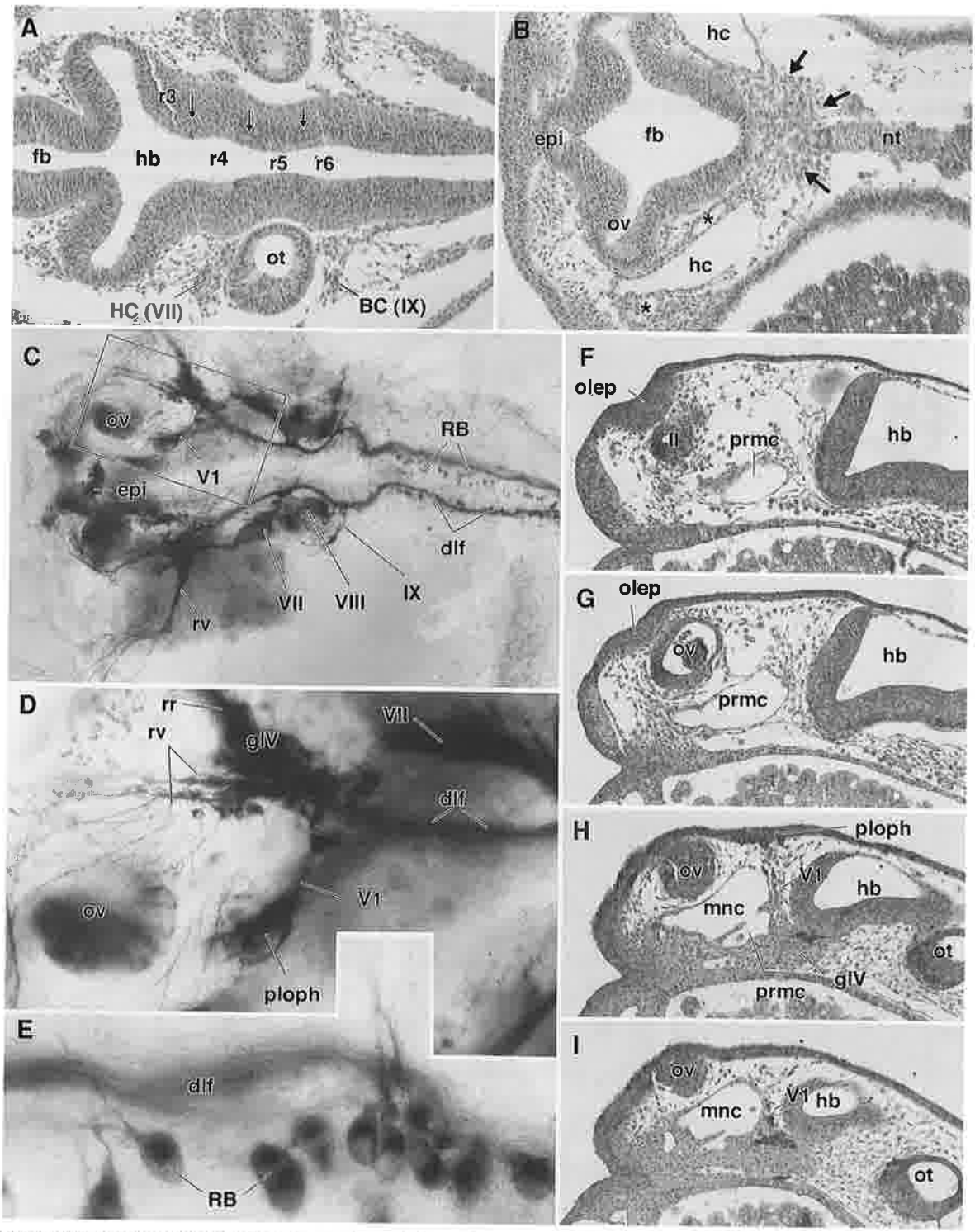

Fig. 4. Histological and immunohistological observations of stage A embryos. **A**: Horizontal section through the anteroposterior axis of the rostral hindbrain. Development of rhombomeric compartments is apparent by neuroepithelial arrangement (rhombomeric boundary levels indicated by arrows). At levels of r2 and r4, putative cephalic crest cell populations (HC, BC) are attached to the meningeal surface of the hindbrain representing facial and glossopharyngeal nerve primordia, respectively. **B**: Another horizontal section from the same embryo as in A, cut through the notochord (nt) and head cavities (hc). Note the dense prechordal mesenchyme distributed between the cavities on both sides and the rostral tip of the notochord (arrows). Asterisks indicate small epithelial cysts associated with the head cavity. **C**: A whole-mount embryo immunochemically stained with HNK-1, seen from the dorsal view. Developing nervous system is stained. **D**: Enlargement of the box in C.[OLE12] Fine neurites are developing from placodal cells. **E**: Enlargement of Rohon-Beard cells in the caudal hindbrain level of the same embryo as shown in C. Neurites of Rohon-Beard cells contribute to the formation of the dorsolateral fasciculus (dlf) or grows laterally into the trunk epidermis. **F–I**: HNK-1-stained histological sections from the same embryo as shown in Fig. 3, which have been cut parasagittally. Sections are arranged in order from medial to lateral levels. Note that premandibular and mandibular cavities are not entirely separated from each other (H).

embryo was the premandibular cavity found in contact with the rostral tip of the notochord, indicating that the mandibular and premandibular cavities arose as a single epithelial cyst simultaneously. No mesodermal epithelial cyst was found caudal to these cavities.

Stage B

Bester embryos hatch between stages A and B (table 1). By stage B, the head cavity had not yet been divided completely (Fig. 5D). The division of the cavities was distinct rostrally, where the two subdivisions showed certain histological differences. Thus, the premandibular portion of the cavity consisted of thicker epithelial cells than that of the mandibular subdivision (Fig. 5C). Furthermore, the lateral cavity was ventrally attached to a dense mesenchyme within the mandibular arch, representing the mandibular arch muscle plate (Fig. 5C,

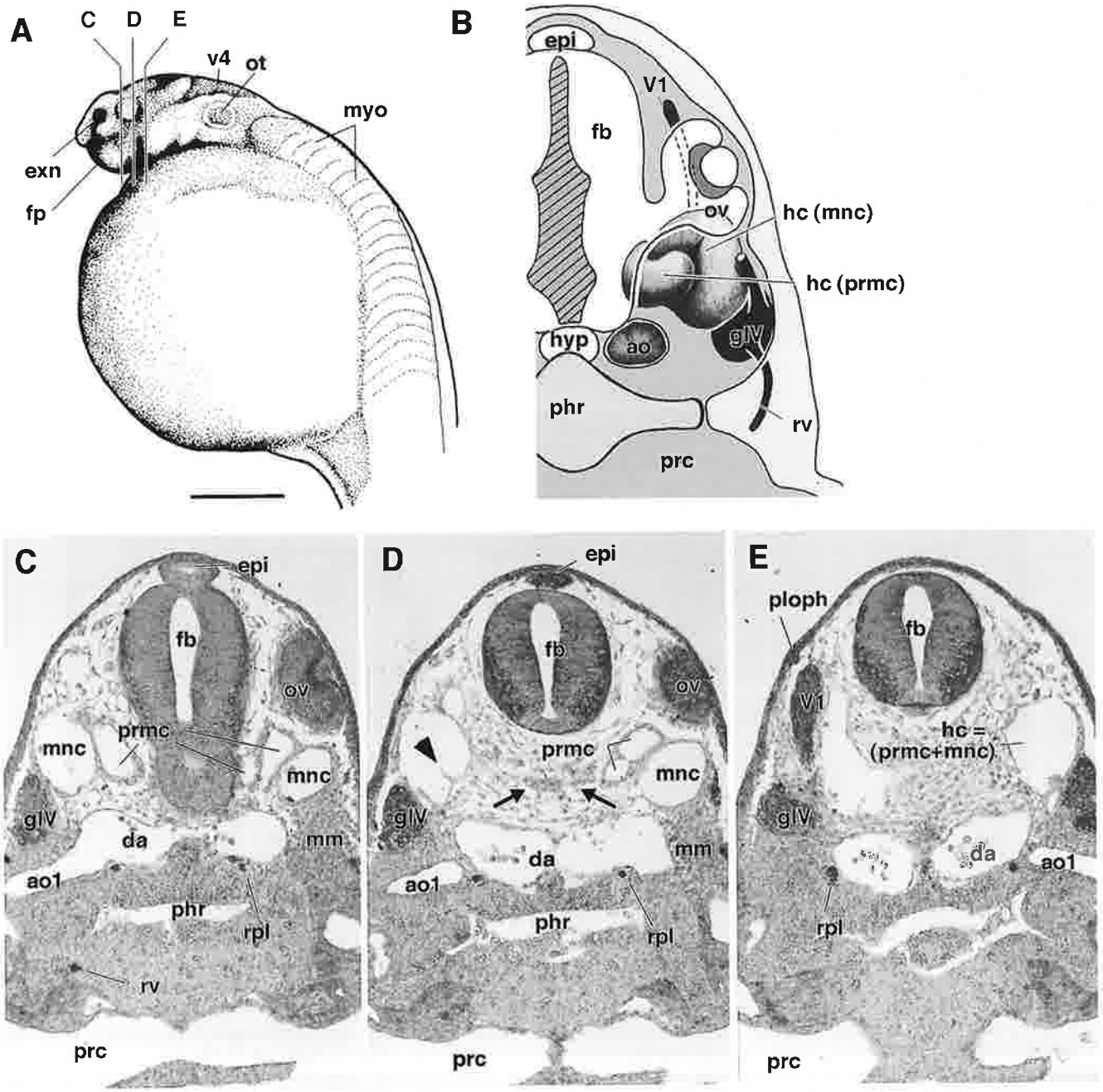

Fig. 5. Stage B embryo. **A**: External morphology of the stage **B** embryo. B: Graphical reconstruction of the head cavity based on transverse sections shown in C to D. Note that the head cavity is mediolaterally subdivided into the premandibular and mandibular cavities. **C–E**: Transverse sections stained immunochemically with the HNK-1 antibody. Note that the division of the head cavities is distinct anteriorly (C), but incomplete caudally (E). Arrowhead in D indicates an indentation in the cavity wall. Arrows in D indicate the premandibular mesenchyme that spans the premandibular cavities on both sides.

D). A similar topographical relationship has been described in elasmobranch (Bjerring, 1977; Kuratani and Horigome, 2000) and lamprey embryos (Kuratani *et al.*, 1999), consistently indicating the homology of this cavity.

In the peripheral nervous system at stage B, the neurite network in the epidermis had developed more extensively in both the head and trunk regions than at stage A (Fig. 6A). In the head, some of the neurites originated from the HNK-1-positive placodal cells scattered in the trigeminal domain (including the profundal region), and many others could be traced to the trigeminal and ophthalmic ganglia. Thus, the contribution from the epidermal placodes was apparent, not only for the profundal, but also for the trigeminal ganglion. Such a scattered distribution pattern of placodes has been observed in the trigeminal domain of various vertebrate embryos (van Campenhout, 1936; Batten, 1957 a, b; Kuratani and Hirano, 1990), which stands in contrast to the so-called epibranchial placodes associated with other branchiomeric nerves (see below).

The profundal nerve still possessed its own nerve root, rostral to the trigeminal nerve root (Fig. 6B). Although the r1/2 boundary was not clear, the close relationship between trigeminal and profundal nerve roots indicates that both issued from r2 (Fig. 6B). The anterior lateral line ganglion first appeared with its own nerve root that connected to the dorsolateral fasciculus at a level slightly caudal to the facial nerve root, and rostral to the acoustic nerve root (Fig. 6A, B). From the facial nerve, the palatine branch grew rostrally beneath the dorsal aorta to a region dorsolateral to the frontal process, where the nerve bifurcated and formed a brush of numerous nerve fibers together with fibers from the rostral branch of the trigeminal nerve (Figs. 5C to E, 6A). Barbel primordia later grew from this place (see below). Since the barbels develop in the maxillary processes of larvae, this trigeminal nerve branch would correspond to the maxillary branch in other vertebrates. In many vertebrate species, the maxillary branch (often called the infraoptic nerve) and palatine branch of the facial nerve form anastomoses in a similar region, where they are involved in the sensory function of the skin (reviewed by Hallerstein, 1933).

Stage C

In stage C, pharyngeal arches 2 and 3 could be distinguished. The position of the second pharyngeal groove corresponded approximately to the level of the otocyst. Beneath the eye and dorsal to the frontal process, there was a swelling on the surface of the larva, indicating the initial development of the barbel (Fig. 6C).

The maxillomandibular prominence became visible on the surface at this stage. The epidermal neurites had diminished as compared with stage B (Fig. 6D, cf. Fig. 6A). An interesting change was recognized in the profundal nerve ganglion, where a new connection had been established with the trigeminal ganglion (Fig. 6D). At this stage and at stage B, epidermal cells showed local staining with HNK-1 antibody, corresponding to the epibranchial placodes. Since the undifferentiated dorsolateral placode was never stained with the same antibody (see below), HNK-1 can be regarded as a reliable marker of epibranchial placodes. As observed in histological sections, however, the placodal contributions to the branchiomeric sensory ganglia were already apparent at stage A (Fig. 3B).

In addition to the palatine branch, the facial nerve at this stage possessed another branch-the post-trematic branch that grew ventrally into the second pharyngeal arch (Fig. 6D).

Stage D

The pectoral fin bud was first observed at this stage. In the head, the maxillomandibular prominence and primordia of the barbels were clearly distinguished on the surface (Fig. 7B). The latter consisted of two pairs of prominences mediolaterally arranged on the future maxillary region (not shown). The dorsal root ganglion was also observed as an HNK-1-positive cell mass in the postotic region (Fig. 7A).

In the cranial nerve, all the epibranchial placodes (geniculate, petrosal and nodose placodes) had appeared on the epidermis as HNK-1-immunoreactive regions dorsolateral to the pharyngeal pouches (Fig. 7A). In the histological section, these placodes were seen as local epidermal thickenings that were in contact with the sensory ganglion primordia of branchiomeric nerves medially (not shown), indicating an active contribution of neuroblasts to these ganglia. From these epibranchial ganglion-placode complexes, as a rule, post-trematic branches grew ventrally into each pharyngeal pouch. That of the facial nerve issued a superficial ramus that also passed ventrally. The rest of the branch was located in a deeper part of the arch, representing the hyomandibular nerve. Distally, it further bifurcated mediolaterally into two ramules, of which the medial branch probably represents the earliest development of the internal mandibular branch or the chorda tympani. The lateral component of the post-trematic branch was the opercular branch.

No pre-trematic branches were apparent in branchiomeric nerves. In addition to the pharyngeal branches, the facial and glossopharyngeal nerves possessed dorsally-growing pharyngeal branches; of these, that of the facial nerve was the palatine nerve, and that of the glossopharyngeal was the dorsal pharyngeal branch (Fig. 7A). Thus, the branchiomeric nerve exhibited typical metameric morphology at this stage.

The most conspicuous change that had occurred by this stage was seen in the profundal nerve. Thus, the nerve had totally lost its own nerve root on the hindbrain (see Fig. 6A, D), and was now connected proximally only to the trigeminal ganglion (Fig. 7A, C). Although the epidermal neurite network had further diminished, the portion that covered the fore-midbrain to the ocular region remained in association with the ophthalmic placode cells. These neurites were connected to the profundal nerve as before.

The lateral line nervous system consisted of components of the anterior lateral line nerve, namely, the superficial ophthalmic and buccal branches as well as the anterior lateral line ganglion, and one middle lateral line nerve component that developed independently at the level of the glossopha-

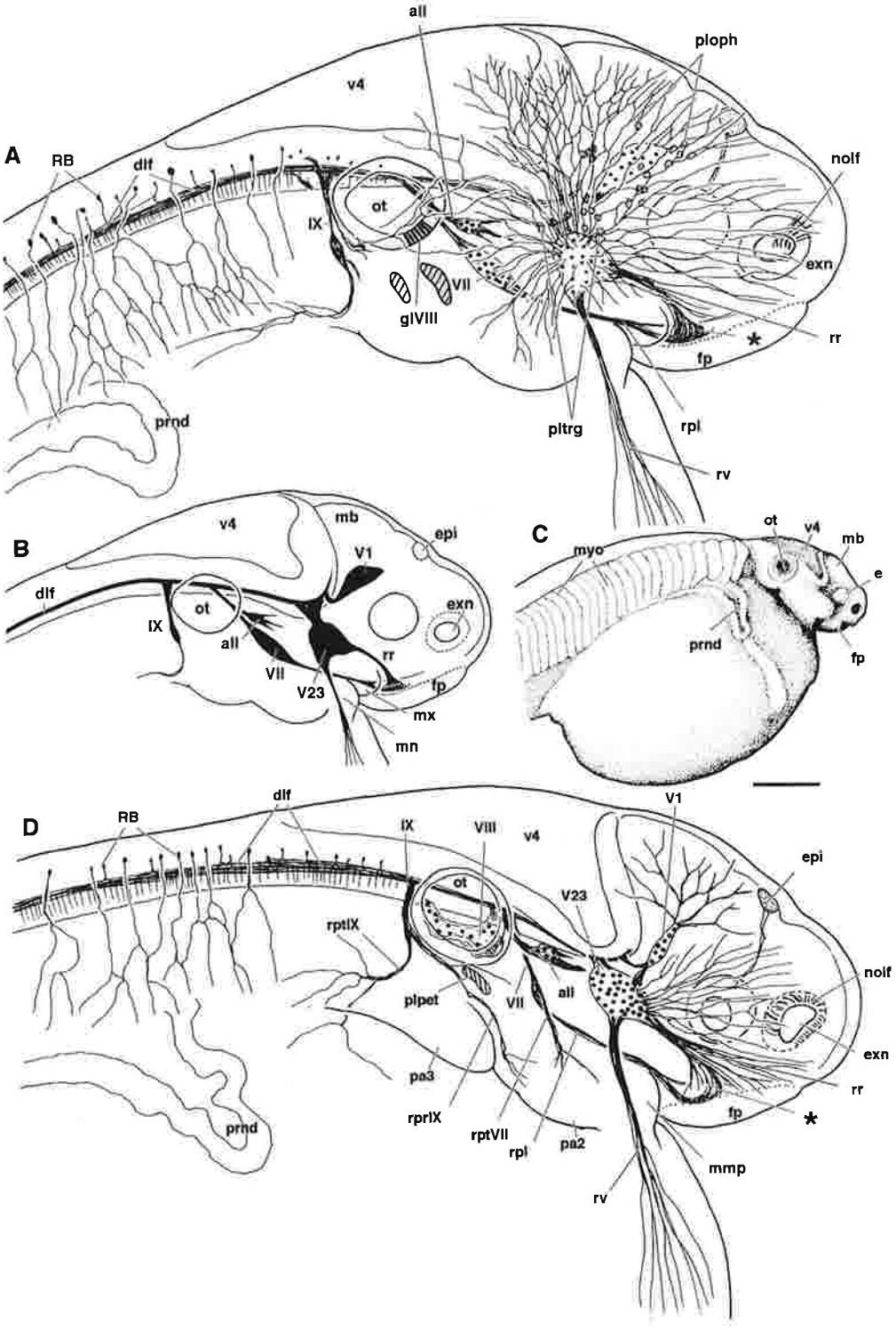

Fig. 6. Peripheral nerve development at stages B and C. **A**: Illustration of a stage B embryo immunochemically stained with HNK-1. Putative sensory ganglia are stippled. Extensive and poorly organized distribution of fine neurites is recognized within the epidermis of the embryo. In the head, the neurites appear to originate from placodal cells (cells labeled "ploph" and "pltrg"), that are also HNK-1-positive and scattered within the epidermis over the trigeminal domain, and those in the trunk from the Rohon-Beard cells (RB). Asterisk (also in D) indicates the nerve network developing in the future barbel. **B**: Schematic illustration of the same embryo as in A. Note that the profundal nerve possesses its independent nerve root on the hindbrain. **C**: External morphology of the Bester embryo at stage C. **D**: Peripheral nerve morphology. Superficial neurites have decreased in number as compared to stage B embryo. Note that the mandibular nerve extends neurites within the epidermis covering the pericardium, far beyond the domain of the mandibular process (mn). Also, note that the profundal nerve (V1) has now established a connection with the trigeminal ganglion (V23). The only lateral line component at these stages is the primordium of the anterior lateral line nerve (all), the nerve root of which has developed slightly rostral to that of the facial nerve (VII). Bar in C=1 mm.

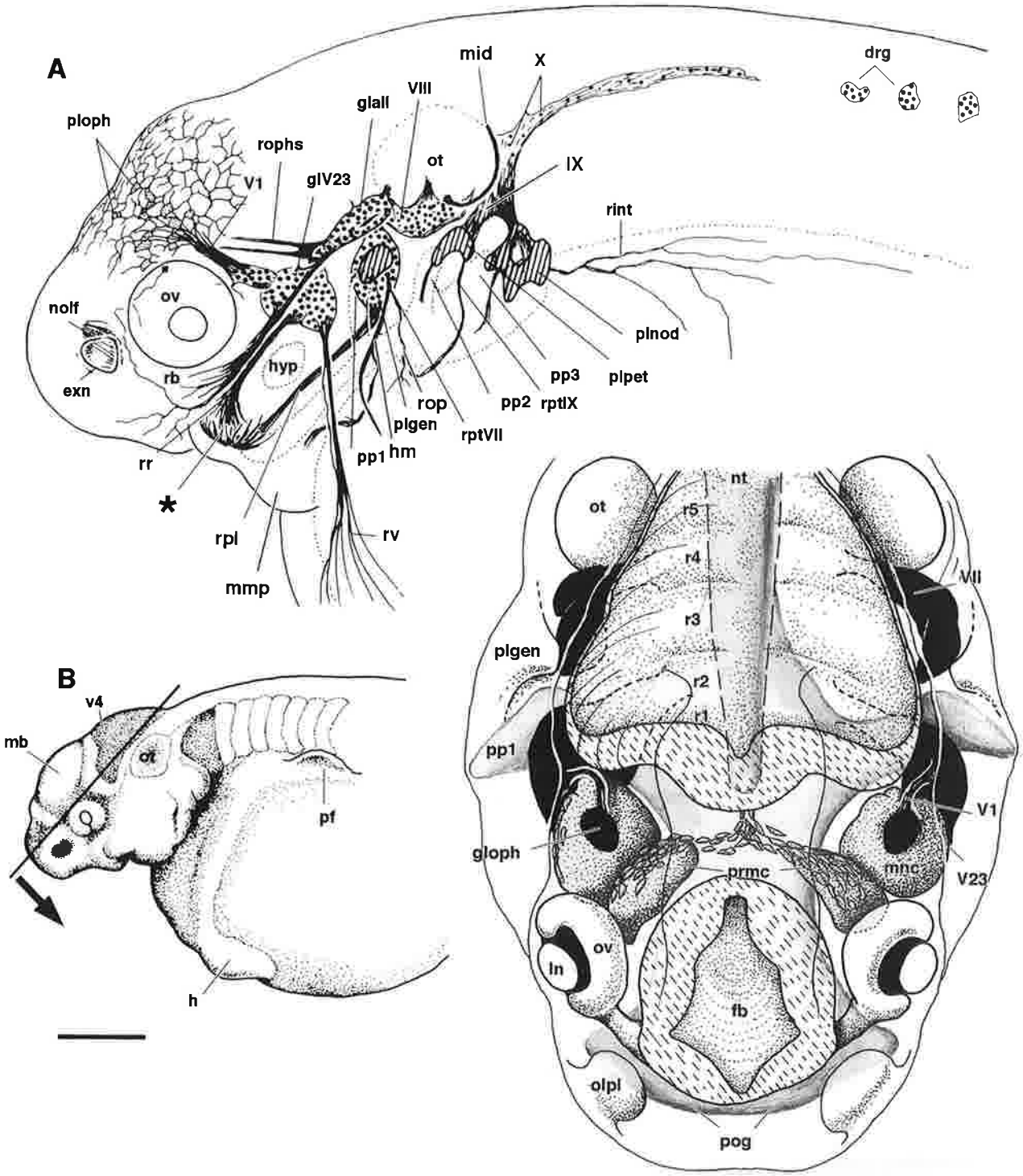

Fig. 7. Stage D embryos. **A**: Peripheral nerve morphology is illustrated based on an HNK-1-immunostained whole-mount specimen. All the placodes have appeared as HNK-1-positive epidermal portions (shaded). Metameric arrangement of branchiomeric nerves is apparent. Most of the immunoreactive neurites have been fasciculated into solid nerve branches. Dorsal root ganglia (drg) are first visible. The superficial neurites have reduced in number, though not entirely disappeared. The Rohon-Beard neurites have also reduced in the trunk, consisting of very fine fibers, which are not illustrated here. Barbel anlage is protruding (asterisk) and receiving numerous nerve processes derived from both trigeminal and facial nerves. Note that the profundal nerve root has disappeared and the nerve has now appeared as a branch of the trigeminal nerve. **B**: External morphology of a stage D embryo. **C**: Graphic reconstruction of a stage D embryo based on histological serial sections. The model is seen from the dorsoanterior view indicated by a line and an arrow in B. Note that the mandibular cavity is situated between the same profundal and trigeminal nerves as stage A (Fig. 3), and that trigeminal and facial nerve roots are located on r2 and r4, respectively. Bar in B=1 mm.

ryngeal nerve (Fig. 7A). The lateral line, innervated by the latter nerve, has been assumed to develop from an independent placode, the middle lateral line placode, in several vertebrates (Northcutt, 1993; see below). The posterior lateral line ganglion was not recognized in the whole-mount embryo. These anterior and posterior components were not yet connected at this stage. Of the anterior lateral line components, the buccal branch consisted of a massive bundle of fibers and possessed a series of short ramules that grew laterally towards the epidermal surface, indicating the innervation of lateral line organs (Fig. 7A).

As observed by graphic reconstruction of the transverse section, the two pairs of epithelial head cavities were now completely separated from each other. As in previous stages, the premandibular cavity was not connected with its counterpart in the middle, and dense mesenchyme still formed a medial bridge between the cavities on both sides. The medial portion of this cell population extended caudally, reaching the rostral tip of the notochord (Fig. 7C). Furthermore, the oculomotor nerve reached the medial part of the cell mass associated with the premandibular cavity (not shown). The distal part of the oculomotor nerve was located between the premandibular and mandibular cavities as seen in elasmobranch and amniote embryos (Goodrich, 1930; Wedin, 1953a,b). The mandibular cavity was located caudolateral to the premandibular cavity, and the ophthalmic ganglion of the trigeminal nerves was situated on the dorsal aspect of the former.

Stage E

On the surface of the embryo, maxillary and mandibular domains were distinguished in the maxillomandibular prominence and the mouth opening was now on the ventral surface of the head (Fig. 8A). The oropharyngeal membrane, however, was not yet ruptured. In addition to the barbel prominence, there was another swelling caudally caused by the development of the anterior lateral nerve ganglion (Fig. 8A, C).

In the brain, the plica encephali ventralis had become even more conspicuous, mainly due to expansion of the hypothalamic region that protruded caudoventrally (Fig. 8B). The telencephalon was well recognized as a separate portion, attached rostral to the dorsal prominence of the diencephalon, or saccus dorsalis (Fig. 8B). Several nerve tracts and commissures were found in the reconstructed specimen, based on the HNK-1-immunostained parasagittal sections. The morphological pattern of the posterior commissure, tracts of habenular, postoptic, and supraoptic commissures were identical to those described in older sturgeon brains (Kupffer, 1906). It was also similar to the nerve tract developmental patterns seen in the embryos of lampreys (Kuratani *et al.*, 1998), teleosts (Wilson *et al.*, 1990; Chitnis *et al.*, 1992), amphibia (Hartenstein, 1993; Burril and Easter, 1994), amniotes (Windle and Austin, 1936; Figdor and Stern, 1993; Windle, 1970; Easter *et al.*, 1993; reviewed by Kupffer, 1906) and Chondrichthyes (Kuratani and Horigome, 2000). The overall morphology of the brain primordium at this stage especially resembled those of Osteichthyes (*Lepidosteus*: Balfour and Parker, 1882; trout: Keibel, 1906; *Amia*: Dean, 1895; *Cyprinus*: Bergquist, 1952; reviewed by von Kupffer, 1906) more than any other classes of vertebrates.

The second pharyngeal arch had begun to grow caudally to form the operculum, and its caudal edge grew external gills (Figs. 8A, 9A). Simultaneously, the original metameric pattern of the branchiomeric nerve was now disturbed. All the epibranchial placodes remained as HNK-1-positive epidermis and the inferior ganglia of branchiomeric nerves were associated with them medially (Fig. 9A). Post-trematic branches of the facial and glossopharyngeal nerves at this stage soon bifurcated anteroposteriorly after they issued from the inferior ganglia, and the anterior sub-branch grew into the deeper part of the pharyngeal arches. Presumably, these deeper branches carried future motor fibers. Immunostaining with MF-20 antibody that recognizes muscle tissue did not show the development of branchial muscles in these arches (Fig. 9C, D).

Most of the major lateral line nerve components had appeared by this stage. The branches belonging to the posterior lateral line nerve (supratemporal and posterior branches) were now recognized, corresponding to the sites of lateral line canals and pit lines described in *Amia* (Allis, 1897). Anterior and posterior lateral line nerves were connected by a communicating branch that developed over the lateral aspect of the otocyst (Fig. 9A). The buccal and communicating branches possessed periodical small ramules to innervate lateral line organs (Fig. 9A). Such a morphological pattern of the early lateral line nerves was clearly observed in whole-mount embryos before the treatment with KOH (Fig. 9B). This reflects the archetype of the dorsolateral placode distribution pattern proposed by Northcutt (1993) and by Northcutt and Brändle (1995). The developmental sites of the superficial ophthalmic and buccal branches corresponded to the anterodorsal lateral line placode, the middle lateral line nerve to the middle, supratemporal branch to the supratemporal, and the posterior lateral line branch to the posterior lateral line placodes, respectively. In *Lampetra*, buccal, superficial ophthalmic and communicating branches are the earliest branches to develop (Kuratani *et al.*, 1997). This is also seen in the shark and some amphibians (*Discoglossus pictus*: Schlosser and Roth, 1995, 1997; *Scyliorhinus torazame*: Kuratani and Horigome, 2000), where buccal and superficial ophthalmic branches develop extremely early among the lateral line nerve branches.

The head cavities had mostly degenerated by this stage, leaving a vestigial epithelial cyst caudal to the eye, surrounded by a dense mesenchyme, presumably derived from this mesodermal epithelium (Fig. 8C). The distal end of the oculomotor nerve had made contact with this cyst, indicating that the latter was the vestigial premandibular cavity (Fig. 8C).

Stage F

The mouth had opened. All the extrinsic eye muscles had clearly developed and no trace of mesodermal coelom or cyst

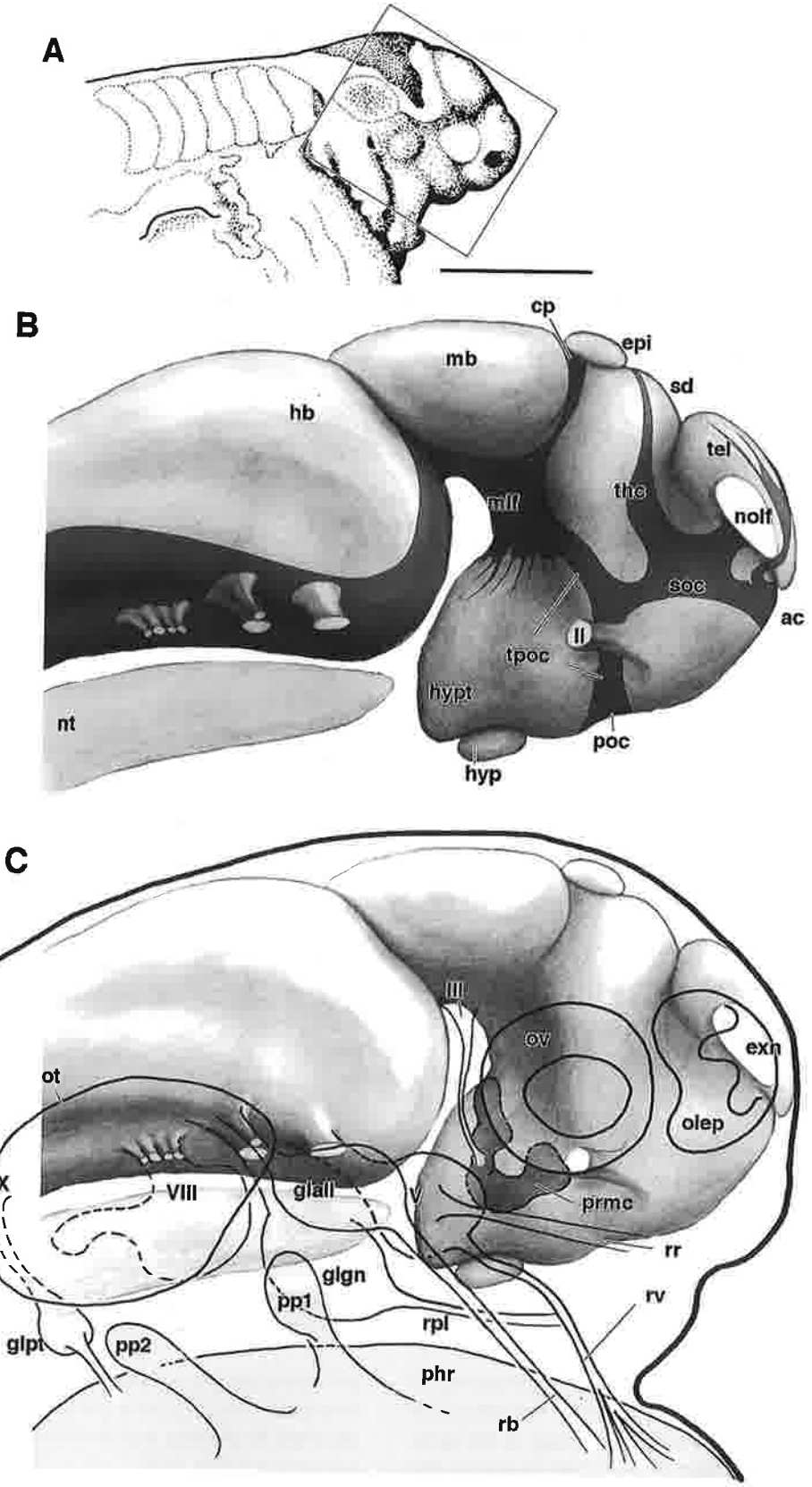

Fig. 8. The nervous system and the head cavity of a stage E embryo. **A**: External morphology. **B**: Reconstruction of the brain based on parasagittal serial sections. Nerve tracts are shaded. **C**: Other embryonic structures are reconstructed and superimposed on the brain. Not all the cranial nerves are indicated. Note that the mandibular head cavity has disappeared and the premandibular cavity diminished. The distal end of the oculomotor nerve is associated with the premandibular cavity. Bar=1 mm.

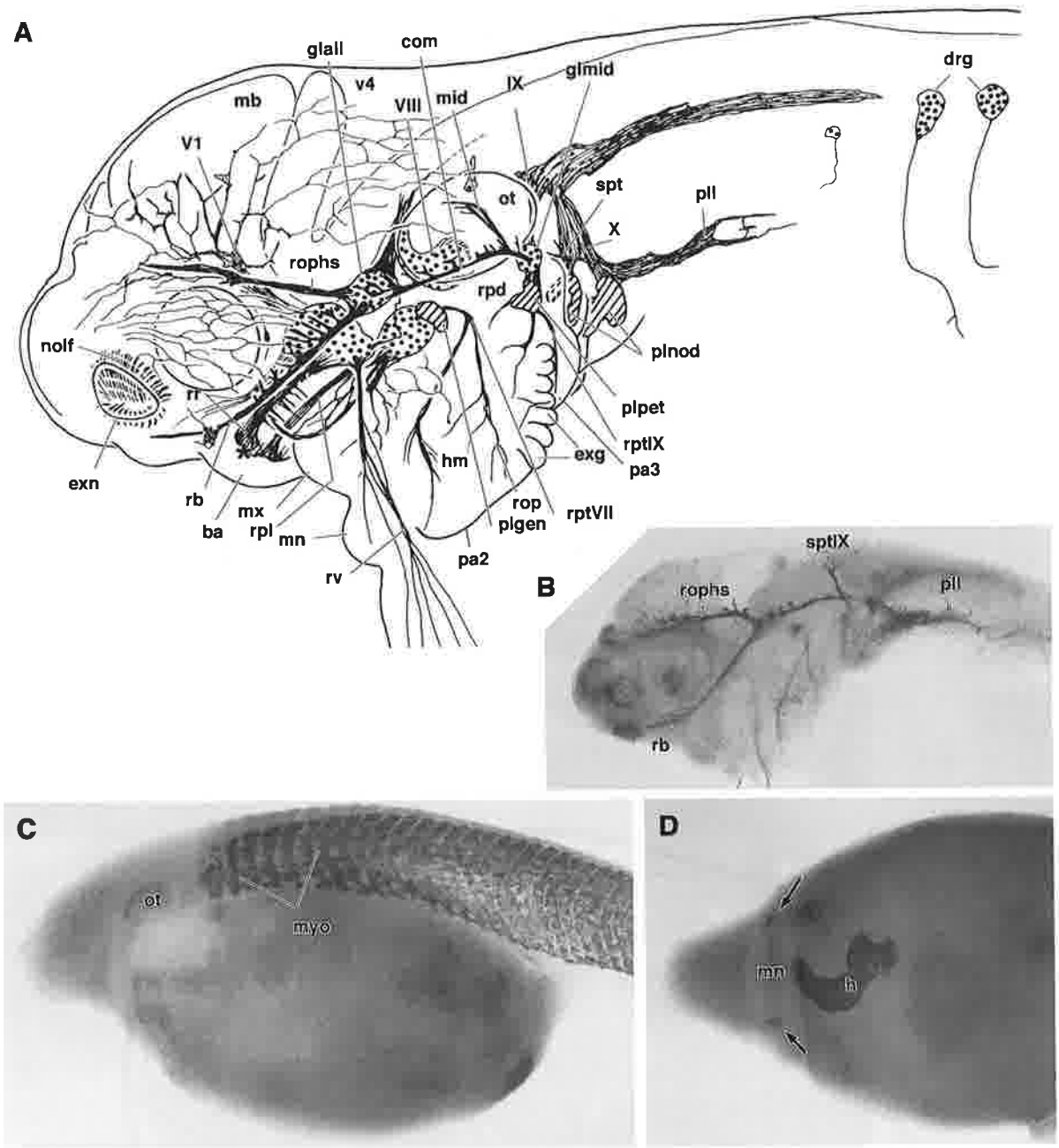

Fig. 9. Stage E embryos. **A**: Peripheral nerve morphology. The second pharyngeal arch has expanded caudally to form the operculum, but the metameric plan of branchiomeric nerve innervation is still apparent. Epibranchial placodes are still present as HNK-1-positive epidermal regions (shaded). **B**: Whole-mount embryo immunochemically stained with HNK-1 antibody. This specimen is not treated with 0.5% KOH, to show the development of the lateral line nerves in a superficial layer of the embryo. **C**: Whole-mount embryo immunochemically stained with MF-20 antibody that recognizes myogenic precursors and muscles. Seen from the lateral view, postotic myotomes are stained. **D**: Same embryo as C, seen from the ventral view. In addition to the heart primordium, a pair of immunostained spots is present at oral angular regions, indicating the development of mandibular adductor muscle.

was found around the eye (not shown). The trochlear nerve could be observed for the first time (Fig. 10B). The amount of yolk had reduced and the external morphology of the larva had now approximated to that of the adult, including the appearance of two pairs of barbels, oral fringes, external nares, an operculum, as well as expansion of the pectoral fins. External gills had developed extensively (Fig. 10A). Although in whole-mount embryos all the epibranchial placodes were still found on the surface ectoderm as HNK-1-immunoreactive areas, the geniculate ganglion had now shifted far medially from its placode and contribution to gangliogenesis was not apparent (Fig. 10B). Concomitant with the modification of the head morphology, as well as the enlargement of the otocyst, the typical peripheral morphology of the facial nerve branches had been somewhat obliterated (Fig. 10B). In the vagus nerve, on the other hand, pre- and post-trematic

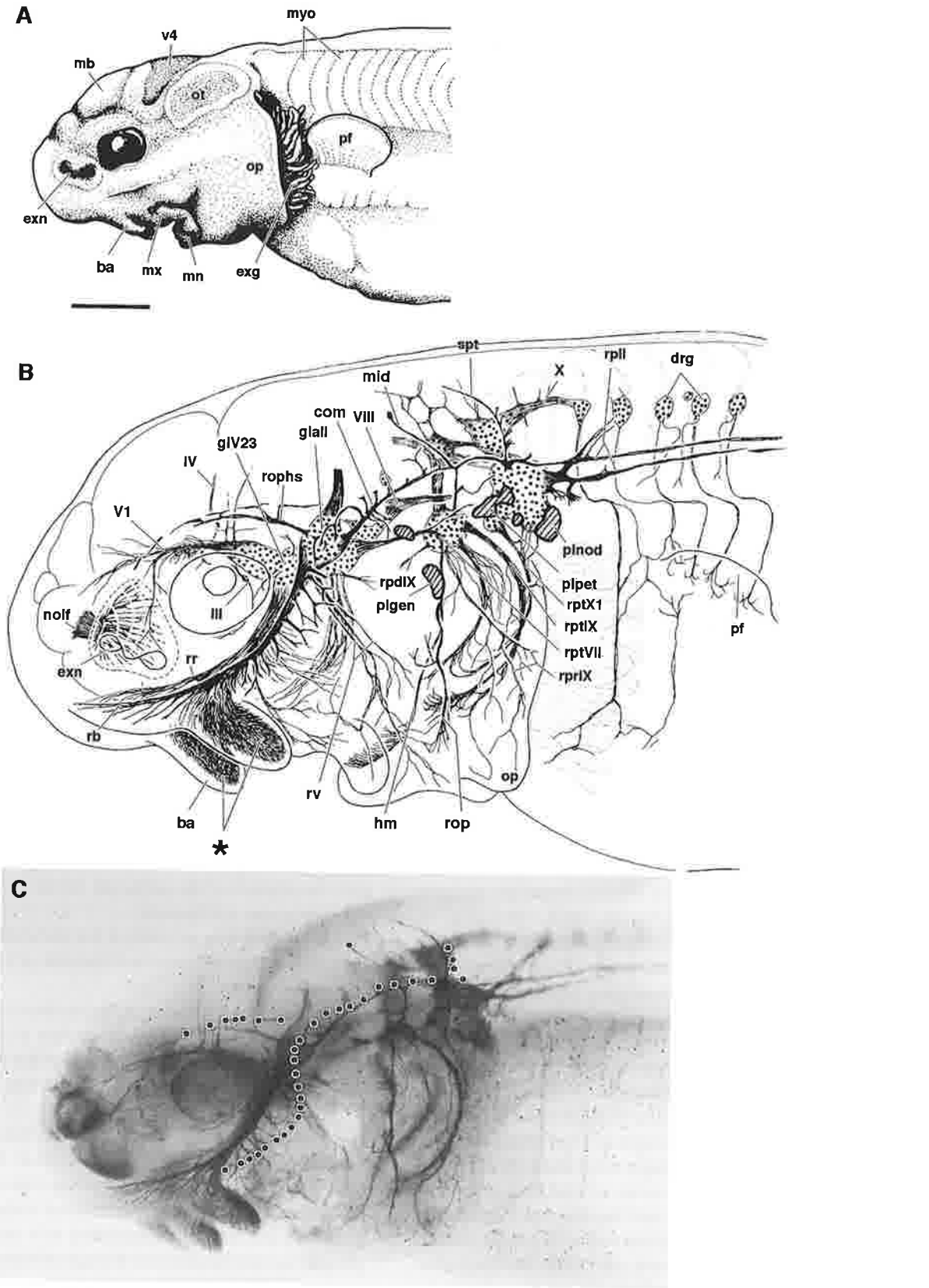

Fig. 10. Stage F embryo. **A**: External morphology. Note the development of the external gill and perioral fringe. **B**: Peripheral nerve morphology. Epibranchial placodes are shaded. Two pairs of barbels have received numerous nerve processes from both the trigeminal and facial nerves. Due to the allometric growth of the head, the metameric plan of the branchiomeric innervation pattern has been disturbed by this stage. **C**: Photograph of the same embryo as illustrated in B. Suggested positions of the lateral line organs are labeled by dots.

branches had appeared in at least two segments (X1 and X2), showing the branchiomeric innervation pattern of the postotic pharyngeal arches (not shown clearly in Fig. 10C).

All the lateral nerve components had appeared, including two supratemporal branches at the levels of the glossopharyngeal and vagus nerves, as well as the posterior lateral line branch that issued from a large ganglionic complex. Ramules for putative lateral line organs were present on most of the branches (Fig. 10B, C). Unlike the anterior lateral line ganglion, the posterior lateral line ganglion could not be seen as an independent cell mass, nor was any independent nerve root for this nerve found in the whole-mount larvae.

In some of the larvae, several rostral spinal ventral rami had formed an extensive distal anastomosis, representing the hypoglossal nerve primordium (not shown in Fig. 10).

DISCUSSION

In the present study, the developing nervous system has been described for the first time using three-dimensional illustrations in staged sturgeon embryos and larvae. Special attention has been paid to the development of mesodermal components (head cavities), neuromeres and neural crest cells, to identify the emerging vertebrate morphotype during development. The process through which the morphological pattern is altered and diverged from the morphotype in the attainment of the characteristic shape of Osteichthyes larvae has also been described.

The HNK-1 antibody appeared to label most of the developing neurons, and it served as a marker especially for epibranchial placodes. This antibody, first generated against human natural killer cells (Abo and Balch, 1982), recognizes a carbohydrate epitope on some cell surface molecules. These epitopes are also reported in neural crest cells of early avian embryos, embryonic neurons and non-neuronal crest cell-derivatives such as glioblasts in various vertebrate embryos (Vincent *et al.*, 1983; Bronner-Fraser, 1986; Holley and Yu, 1980; Sadaghiani and Vielkind, 1990; Nordländer, 1989, 1993; Covell and Noden, 1989). Immunoreactivity to this antibody appears to be restricted to developing neurons, at least in amphibian, rat, zebra fish, and lamprey embryos (Nordländer, 1989, 1993; Metcalfe *et al.*, 1990; Kuratani and Bockman, 1992; Kuratani *et al.*, 1997; unpublished observation). In a late pharyngula of a *Scyliorhinus*, as in the chick, HNK-1 marked not only neurites, but also putative crest cell-derived Schwann cells along the PNS (unpublished observation). In the Bester, glial cells did not seem to be labeled by this antibody, and this animal is likely to be counted as another species for which HNK-1 serves as the neuronal marker. This antigen is also known as one of the earliest neuronal markers in zebra fish and *Xenopus* (Nordländer, 1989, 1993 and references therein; Metcalfe *et al.*, 1990). This also appears to be the case with the Bester, from the extensive labeling seen of nerve tract and peripheral fibers. Thus, the immunostaining methods employed in the present study seem suitable for detecting the developing nervous system in the Bester. In the following discussion, the developmental morphology of the Bester embryo will be dealt with in the context of comparative embryology and developmental biology.

Several embryonic features of Bester-comparative embryology

In Bester embryogenesis, several morphological characters were recognized to constitute the vertebrate morphotype, or the primitive set of features commonly shared by various vertebrate species. These are:

(1) basic brain components and stereotyped tract formation;
(2) rhombomeric segmentation of the hindbrain;
(3) segmental attachment of crest cell populations onto even-numbered rhombomeres to form branchiomeric nerve roots;
(4) metameric distribution pattern of crest cell populations within pharyngeal arches;
(5) postotically restricted development of myotomes;
(6) possession of typical lateral line nerve morphology;
(7) scattered pattern of trigeminal and profundal placodes;
(8) epibranchial placodes as focal thickenings of epidermis.

Compared with other major groups of vertebrates, several aspects of Bester embryonic development were rather specific to Osteichthyes, or possibly to sturgeons. These include:

(9) caudal position of the rostral tip of the notochord;
(10) late appearance of the mandibular arch;
(11) laterally expanded head over the yolk at early pharyngula;
(12) the frontal process of the forebrain;
(13) development of head cavities from a common epithelial anlage;
(14) lack of the hyoid cavity;
(15) conspicuous plica encephali ventralis;
(16) early protrusion of the saccus dorsalis (parencephalon);
(17) long-lasting processus neuroporicus;
(18) the position of the profundal nerve and ganglion within the cavum epiptericum;
(19) secondary loss and shift of the profundal nerve root;
(20) early extensive epidermal neurites of placodal neurons in the head;
(21) early epidermal neurite of Rohon-Beard cells in the trunk;
(22) caudal expansion of the operculum at larval stages and modified peripheral morphology of the facial nerve;
(23) innervation of the barbel by trigeminal and facial nerve branches.

Many of the above listed features, those numbered 11, 12, 15–18, 20–22, are shared by other Osteichthyes as already noted, indicating the possibility that bony fish develop on the basis of a specifically conserved body plan among the group. Character 18 is associated with several vertebrate groups, but may be obtained through different developmental processes. Character 21 is also found in lamprey, elasmobranch and amphibian embryos, and may represent a very primitive neural developmental pattern of vertebrates (see below). Developmental patterns of mesodermal head cavities (13, 14) are very problematic. Widely spread knowledge about

the head mesodermal segmentation is still strongly influenced by descriptions on embryonic elasmobranchs, and developmental sequence of head cavities has not been scrutinized with the exception of several amniotes (Adelmann, 1925, 1926). Evaluation of this structure is profoundly associated with the origin of the vertebrate head itself.

Neural crest cells, rhombomeres and peripheral nerves in Bester embryos-vertebrate morphotype in embryogenesis

Neural crest cells give rise to a variety of cell types and play fundamental roles in the head morphogenesis. They migrate along the dorsolateral pathway beneath the epidermis, forming several discrete cell populations of ectomesenchyme as the bases for craniofacial patterning. The crest cells in each pharyngeal arch also form branchiomeric nerve primordia in a segmental fashion with their nerve roots attached on even-numbered rhombomeres of the hindbrain (Coghill, 1916; Tello, 1923; Kuratani, 1991; Köntges and Lumsden, 1996; reviewed in Kuratani *et al.*, 1999). The metamerism of branchiomeric nerves, therefore, offers developmental bases in early embryogenesis as represented by crest cell migration and neuroepithelial compartmentalization in the mid-hindbrain region. The epibranchial placodes are also a segmental embryonic component of the branchiomeric nerves, contributing neuroblasts to the formation of the sensory ganglia (reviewed by Noden, 1992).

The earliest stage observed in the present study corresponded to early pharyngula (Fig. 2B), in which neural crest cells had already attained a typical distribution pattern in the head. In the histological sections and graphic reconstructions, the cephalic crest cells were distributed beneath the surface ectoderm, apparently having migrated along the dorsolateral pathway as in various vertebrates (Horigome *et al.*, 1999 and refs. therein). It can be clearly seen that each crest cell streams into each pharyngeal arch (Fig. 2B) prefigured peripheral morphology of the branchiomeric innervation pattern, which is also metameric at early larval stages (Figs. 7, 9).

Branchiomeric nerve root-rhombomere relationships are also established by stage A, whereby the trigeminal nerve root is found on r2, the facial nerve root on r4, and the glossopharyngeal nerve root on r6. This segmental assignment seems to remain at least until stage D (Fig. 7A), and further morphology of the PNS indicates that the rhombomeric position of the nerve roots is fixed throughout development (see below). Although the peripheral part of the lateral line nervous system appears independent of this rhombomeric system, its central connection or root formation definitely follows the nerve ports on even-numbered rhombomeres (Figs. 6, 7, 9, 10).

Morphology of rhombomeres is less clear in Bester than in amniote and shark embryos; the meningeal surface of the hindbrain never showed segmental boundaries, although weak boundaries were observed at stage D on the apical surface (Fig. 7C). In young embryos also, rhombomeres are apparent only by disposition of nuclei; intrasegmental neuroepithelial cells are arranged in a fan-shape that expands laterally (Fig. 4A), typical of rhombomeres in various vertebrates (Orr, 1887; Vaage, 1969; reviewed by Lumsden and Keynes, 1989).

Not only developmentally, but also anatomically, the branchiomeric nerves of sturgeons have been known to exhibit metameric organization. In the adult anatomy of *Acipenser ruthenus*, each of the branchiomeric nerves has been illustrated to possess the same sets of nerve branches by Sewertzoff (1911). As a rule, the inferior ganglion sends pre- and post-trematic branches ventrally along rostral and caudal aspects of the gill slits, and another rostrally-oriented branch (dorsal pharyngeal branch) that further bifurcates distally into dorsal and ventral branches. The latter nerve is also often called the pre-trematic branch (reviewed by Hallerstein, 1934). In the present study, not all of these branches were recognized in developing embryos and larvae. Nevertheless, the post-trematic branch was often seen as the earliest branch to develop in every branchiomeric nerve (Fig. 9). Of these branches in the pharynx, those belonging to the facial nerve seemed to undergo the most profound modification due to the expansion of the operculum as well as to the innervation of the barbel by its palatine branch.

In the sturgeon, the operculum develops rapidly during larval stages and it covers all the postotic pharyngeal arches (Fig. 10). Such a condition, however, is temporary. The caudal growth of the arches exceeds that of the operculum in later development. Thus, the metameric morphology of the branchiomeric nervous system is regained in the adult morphology as illustrated by Sewertzoff (1911). The branchiomeric nature of the profundal and trigeminal nerves was not evident in any stage of Bester embryos. This may partly be due to the highly modified mandibular arch in the early state of this animal, as well as the formation of the frontal process and expanded peri- and preoral regions (Figs. 2B, 3B).

Early developmental pattern of sensory neurites

One of the greatest advantages of whole-mount immunostaining of the nervous system is that the three-dimensional morphology of fine ramules or fibers can be observed easily (Ishikawa *et al.*, 1986; Kuratani *et al.*, 1997; Schlosser and Roth, 1995, 1997). Most of such structures are unable to be reconstructed from serial histological sections, especially in small embryos. In the early phase of peripheral nervous system (PNS) development, Bester embryos show an extensive neurite outgrowth in the head and trunk regions. The innervation of the head epidermis is exclusively by trigeminal and profundal sensory neurons and they are very probably of placodal origin. Unlike the more posterior placodes (geniculate, petrosal, and nodose placodes) that consist of HNK-1-positive ectoderm, those of trigeminal and profundal nerves are scattered on the surface ectoderm and grow neurites *in situ*. This type of early neurite growth was not seen in shark embryos (*Scyliorhinus torazame*: Kuratani and Horigome, 2000; *Cephaloscyllium*: unpublished observation), but is common to all teleosts that we have observed so far (zebra fish, cat fish, unpublished observations).

The superficial neurites in the trunk originate from Rohon-

Beard cells that also appear to contribute to the dorsolateral fasciculus intramedullarly (Fig. 4C, D). Similar neurites also develop in the shark embryos (Kuratani and Horigome, 2000) and in embryos of indirect developing frogs (*Discoglossus pictus*: Schlosser and Roth, 1995, 1997). In larvae of the lamprey (*Lampetra japonica*) that burrow in the mud after hatching, superficial neurites develop in the trunk epidermis at early stages (Kuratani *et al.*, 1997). The early development of Rohon-Beard cells has been described in several aquatic forms (Spitzer and Spitzer, 1975; Lamborghini *et al.*, 1979) and they have been shown physiologically and anatomically to function as primary sensory neurons (Coghill, 1914; Hughes, 1957; Spitzer and Baccaglini, 1975, 1976; Baccaglini and Spitzer, 1977). Such a function, however, seems to be a temporary adaptation, and the neurons have been observed to disappear early in larval life (Hughes, 1957). It seems likely that these placodal neuritis, as well as those of Rohon-Beard cells, are early larval adaptations to post-hatching sensory functions, before the establishment of the lateral line system in larvae of Osteichthyes. Although this should also be tested electrophysiologically in Bester embryos, the concept is plausible, since the network became most extensive around the time of hatching (at stage B) and then reduced as the lateral line nerve began to appear. The regression of Rohon-Beard cells, concomitant with the appearance of dorsal root ganglia that begins at stage D (third larval day), is consistent with the report in *Acipenser* in which these cells entirely disappear on the ninth larval day (reviewed by Nieuwenhuys, 1997). In the present study, Rohon-Beard cells were scattered along the spinal region at stage E (4 to 5 days after hatching). The above assumption, however, does not always explain the presence of Rohon-Beard neurites in shark embryos that stay in the egg shell until the completion of the adult form.

Morphologically, the above-noted early epidermal neurites exhibit several interesting features. First, Rohon-Beard neurites grow roughly in a dorsoventral, but poorly organized direction; no segmental pattern is apparent as in late-developing spinal nerve branches. Such a morphological trait is reminiscent of those in the shark and teleost embryos (Kuratani and Horigome, 2000; unpublished observation). The trigeminal neurites also lack an embryonic domain-restricted innervation pattern. Those neurites originated from the trigeminal ganglion extend caudally as far as the level of the otocyst or even beyond it, and rostrally cover the eye and the perinasal region (Fig. 6). Similarly, the mandibular branch grows far beyond the domain of the mandibular arch covering the anterior aspects of the yolk sac. In the development of the shark and amniotes, the early development of the cranial nerve branches proceeds in parallel with the migration or distribution of the crest cells, leading to a stereotyped innervation pattern (see Johnston, 1966; Kuratani and Tanaka, 1990). Probably, growth of the temporary epidermal neurites in early Osteichthyes larvae is independent of the mesenchymal prepattern.

Head cavities and peripheral nerves in the sturgeon

In the embryonic head of various vertebrates, several epithelial mesodermal segments are known to develop before differentiation of extrinsic eye muscles (Balfour, 1878; van Wijhe, 1882; Fraser, 1915; reviewed by Goodrich, 1930; Brachet, 1935; Wedin, 1949; Jarvik, 1980; and by Jacob *et al.*, 1984). Typically, three pairs of head cavities have been described in Chondrichthyes embryos termed, from anterior to posterior, the premandibular, mandibular, and hyoid cavities, respectively. Similar subdivision of the head mesoderm is also seen in the lamprey embryo, although it does not lead to the secondary formation of an epithelial anlage in this animal (Kuratani *et al.*, 1999). In many amniotes, on the other hand, epithelial cysts often develop in association with the extrinsic eye muscle development (Adelmann, 1925, 1926; Fraser, 1915; reviewed by Brachet, 1935). The presence of head cavities, therefore, does not necessarily represent a primitive character of vertebrates, but is rather secondarily acquired in gnathostomes. In a few sharks, another unpaired head cavity, Platt's vesicle, has been recognized in front of the premandibular cavity (Platt, 1891). This cavity, from its fate and morphology, is now regarded as part of the premandibular cavity (see Jefferies, 1986; reviewed by Kuratani *et al.*, 1999).

Segmental appearance of head cavities does not represent anteroposterior segmentation of paraxial mesoderm in a manner similar to trunk somites, but the division appears to be brought about by epigenetic influences from surrounding structures (Kuratani *et al.*, 1999). Basically, the three head cavities develop from the prechordal mesoderm in a caudal to rostral direction, and the last cavity to develop, or the premandibular cavity, remains unpaired, each counterpart connected in the middle to which the rostral tip of the notochord is attached (Fig. 11 above).

In the present study, Bester embryos were observed to develop two pairs of head cavities. From their positions, the rostromedial pair was identified as the premandibular, and the caudolateral ones as mandibular cavities, although their developmental fates were unable to be determined. Association of the oculomotor nerve also confirms the identity of the premandibular cavity (Fig. 8C). Unlike the report of Ostroumow (1906), no epithelial mesoderm representing the hyoid cavity was found in Bester embryos caudal to the mandibular cavity.

Morphological similarity of the mandibular and premandibular cavities in Bester to the same named cavities in the shark is not superficial; the mandibular cavity in Bester lies between the profundal and trigeminal nerves as seen in the shark (Kuratani and Horigome, 2000). The same topography is only temporarily present in the lamprey embryo (Damas, 1944; Kuratani *et al.*, 1999). The Bester premandibular cavities on both sides are connected by a dense mesenchyme that expands from an overt rostral tip of the notochord (Fig. 2B, 3, 7C). This mesenchyme is most probably derived from the prechordal plate in early development (Fig. 11). Interestingly, however, such homologies of head cavities do not seem to depend upon identical developmental processes between

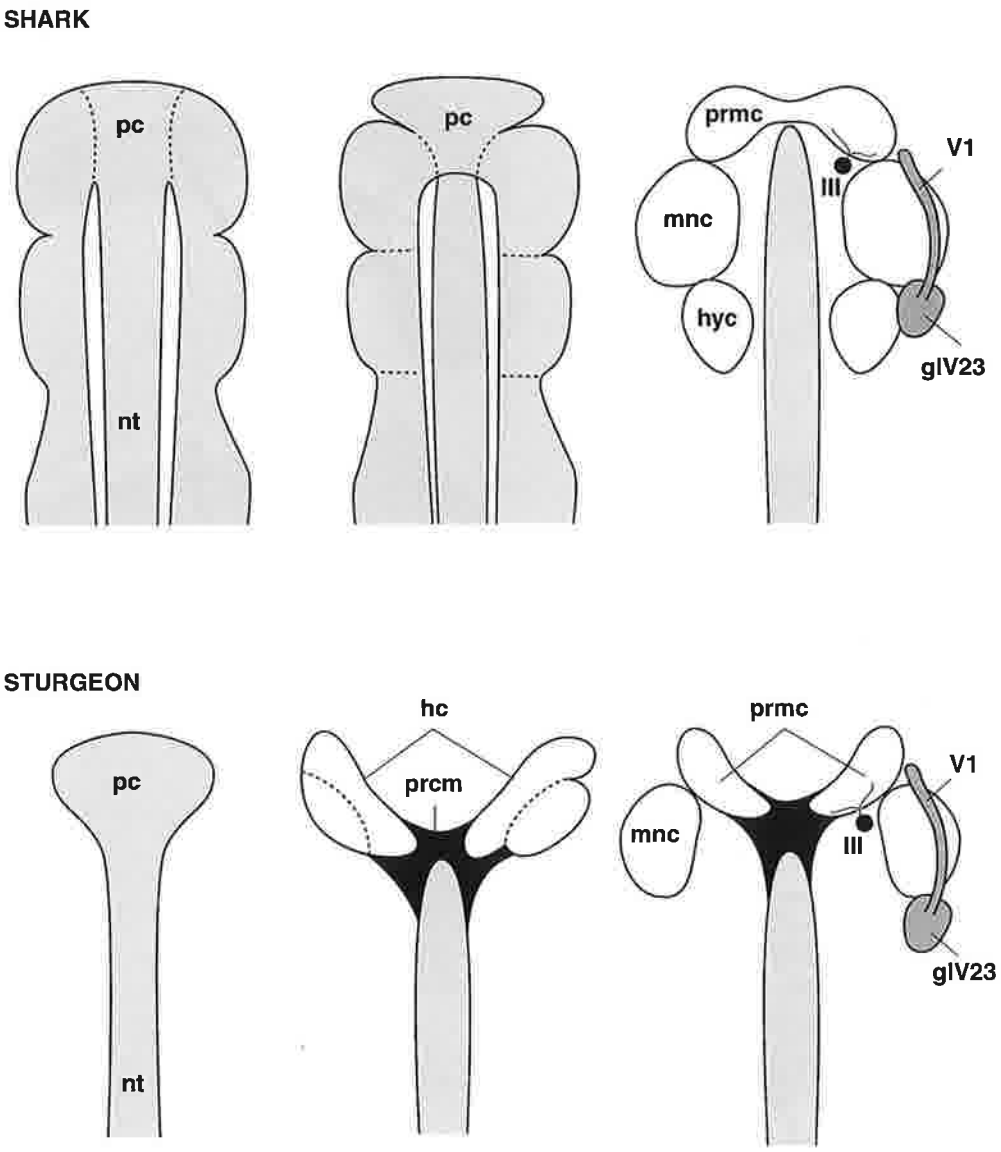

Fig. 11. Developmental sequences of the head cavity in the shark and sturgeon. In the shark, development of the head mesoderm and head cavity proceeds from caudal to rostral sequence as a part of acrogenesis (head formation). Much of the head mesodermal components arise from the rostral mesodermal source, the prechordal plate, which also gives rise to the most rostral portion of the notochord. In sturgeon development, on the other hand, a pair of well-epithelialized head cavities appears first, which are secondarily subdivided mediolaterally into two pairs of cavities.[OLE14] From the topographical relationships with cranial nerves (oculomotor nerve, III; profundal nerve, V1; trigeminal ganglion, glV23) and other structures, these two cavities are identified as premandibular and mandibular cavities, respectively. The hyoid cavity never appears in the sturgeon embryo.

sharks and sturgeons. In the Bester embryo, both of the above head cavities appear as a common single pair of epithelial mesoderm at stage A (Fig. 11 below). At this stage, the cavities on both sides are already connected by the prechordal mesenchyme (Fig. 2B). This cavity is soon divided into two components mediolaterally, each subdivision representing the premandibular and mandibular cavities, respectively. The division is irregular and incomplete at first: the intermediate state of division is seen at stages A to C (Figs. 3, 5). For one possible explanation, it could be that epithelial swelling of the head cavity precedes the caudal to rostral segmentation of the mesoderm in Bester development. It is also probable that, regardless of diversified mesodermal cell lineages, a similar embryonic environment imposes similar regionalization of the cephalic mesoderm, which maintains the conserved association with the same cranial nerves among vertebrates.

In the development of a shark, *Scyliorhinus torazame*, we previously assumed that developmental shift of branchiomeric nerve roots along the neuraxis (trigeminal nerve root moves from r2 to r3) may possibly be due to fixed relationships between nerves and head cavities, and simultaneous allometric growth of the brain (Fig. 12; Kuratani and Horigome, 2000). In the Bester embryo, degradation of head cavities proceeds relatively rapidly and the cavity does not appear to push

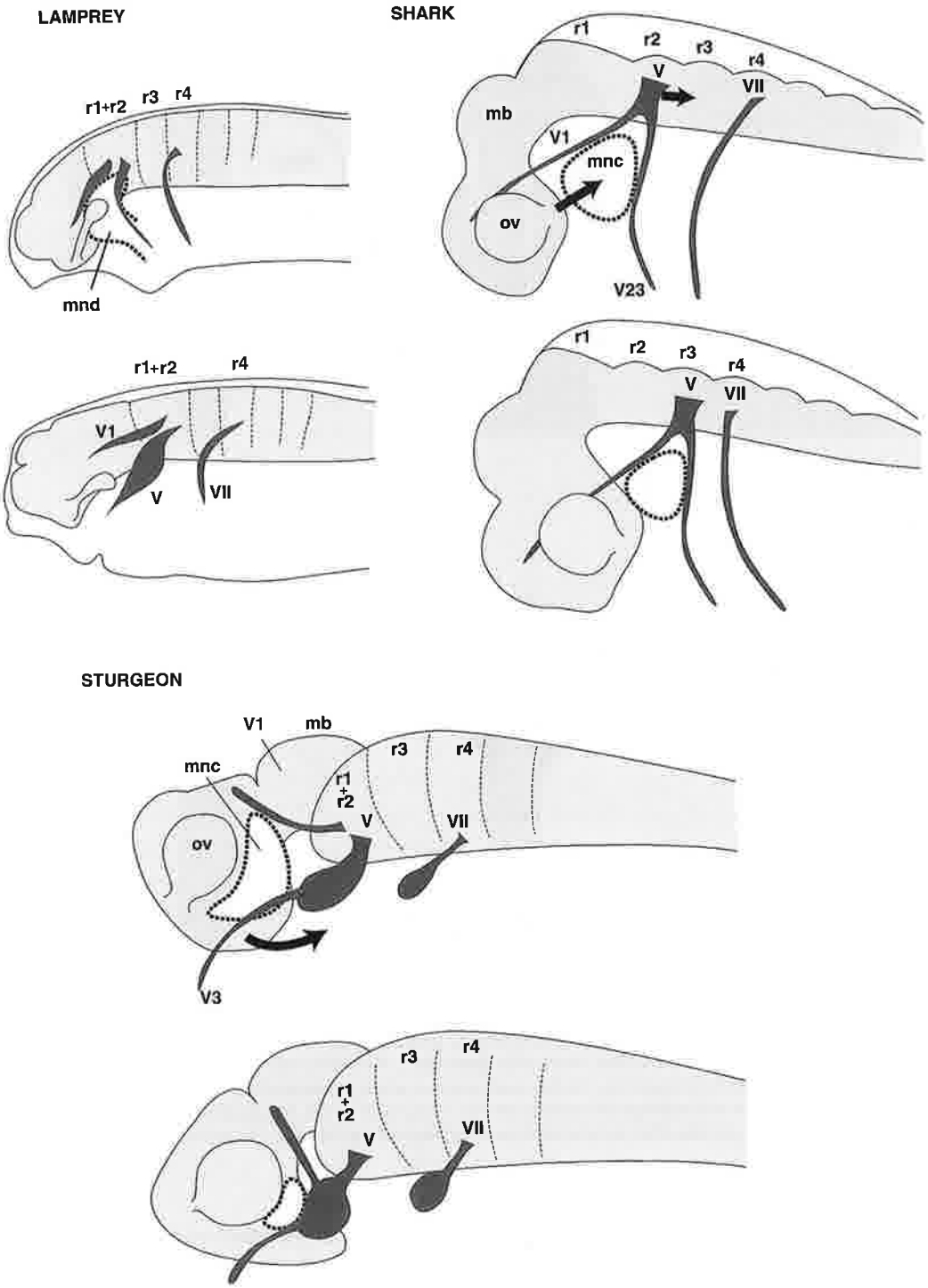

Fig. 12. Topography of cranial nerves with head cavities. Heterochronic and heterotopic differences in embryogenesis may epigenetically affect the anatomical topography of the nervous system in various ways. In the lamprey (above, left), the mandibular mesoderm never forms the epithelial cavity, and the common nerve-mesoderm topographical relationships are only seen at early stages. In the shark (above, right), relatively large head cavities appear in pharyngula and remain for a long period of development, during which, plica encephali ventralis develops gradually and concomitantly the forebrain grows caudally. This process continuously pushes the mandibular cavity caudally together with the trigeminal nerve root, which may explain the caudal shift of the trigeminal nerve root from r2 to r3 level (Kuratani and Horigome, 2000). In the sturgeon development (below), on the other hand, plica encephali ventralis is already well-developed at early pharyngula. Although the mesodermal and nerve elements arise in shared topographical relationships as in the shark, the early degeneration of the head cavity does not affect the position of the trigeminal nerve root on the hindbrain.

the trigeminal nerve root caudally. At stage D, when the head cavities are most clearly seen (Fig. 7C), the trigeminal nerve root is fixed on r2, and further modification of cranial nerves seems to occur in the periphery (Figs. 9, 10). The same nerve-rhombomere relationships are retained in the lamprey, since head mesoderm barely imposes any burden on peripheral nerve patterning (see above; Fig. 12).

ACKNOWLEDGMENTS

The MF-20 antibody developed by Dr. D. A. Fishman was obtained from the Developmental Studies Hybridoma Bank maintained by the Department of Pharmacology and Molecular Sciences, Johns Hopkins University School of Medicine, Baltimore, MD 21205, and the Department of Biological Sciences, University of Iowa, Iowa City, IA 52242, under contract N01-HD-6-2915 from the NICHD. We are grateful to Yukito Katsumi and Kiyoshi Hiraoka in Fujikin Co. Ltd., Tsukuba City, Ibaragi Prefecture, Japan, for providing Bester embryonic materials, to Hiroyuki Takeda at Nagoya University and Midori Kobayakawa at Kyushu University for the gift of some teleost embryonic specimens, and to Naoto Horigome, Shinnya Watanuki, and Miyoko Myojin for technical assistance. We also thank Edwin Gilland for communicating his unpublished observations and valuable discussions. Sincere gratitude is extended to Shigenori Tanaka for his valuable comments on the manuscript. This work was supported by grants-in-aid from the Ministry of Education, Science and Culture of Japan.

REFERENCES

Abo T, Balch CM (1982) Characterization of HNK-1 (Leu-7) human lymphocytes. II. Distinguishing phenotypic and functional properties of natural killer cells from activated NK-like cellls. J Immunol 129: 1758–1761

Adelmann HB (1925) The development of the neural folds and cranial ganglia of the rat. J Comp Neurol 39: 19–127

Adelmann HB (1926) The development of the premandibular head cavities and the relations of the anterior end of the notochord in the chick and robin. J Morphol 42: 371–439

Allis EF (1897) The anatomy and development of the lateral line system in *Amia calva*. J Morph 2: 487–808

Baccaglini OI, Spitzer NC (1977) Developmental changes in the inward current of the action potential of Rohon-Beard neurones. J Physiol 271: 93–118

Balfour FM (1878) The development of the elasmobranchial fishes. J Anat Physiol 11: 405–706

Balfour FM, Parker WM (1882) On the structure and development of *Lepidosteus*. Phil Trans Roy Soc 2: 359–441

Batten EH (1957a) The activity of the trigeminal placode in the sheep embryo. J Anat 91: 174–187

Batten EH (1957b) The epibranchial placode of the vagus nerve in the sheep. J Anat 91: 471–489

de Beer GR (1922) The segmentation of the head in *Squalus acanthias*. Quart J microsc Sci 66: 4578–474

de Beer GR (1924) The prootic somites of *Heterodontus* and of *Amia*. Quart J microsc Sci 68: 17–38

Bergquist H (1952) Studies on the cerebral tube in vertebrates. The neuromeres. Act Zool Stockholm 33: 117–187

Bjerring HC (1977) A contribution to structural analysis of the head of craniate animals. Zool Scrpt 6: 127–183

Bolker JA (1993) The mechanism of gastrulation in the white sturgeon. J Exp Zool 266: 132–145

Bond CE (1996) "Biology of Fishes" 2nd ed, Saunders College Publishing, Fort Worth

Brachet A (1935) "Traité d'Embryologie des Vertébrés" Masson & Cie, Etiteurs, Paris

Bronner-Fraser M (1986) Analysis of the early stages of trunk neural crest migration in avian embryos using monoclonal antibody HNK-1. Dev Biol 115: 44–55

Burril JD, Easter SS Jr (1994) Development of the retinofugal projections in the embryonic and larval zebrafish (*Brachydario rerio*) J Comp Neurol 346: 583–600

van Campenhout E (1936) Contribution a l'étude l'origine des ganglion des nerfs craniens mixtes chez le porc. Arch Biol 47: 585–605

Chitnis AB, Patel C K, Kim S, Kuwada JY (1992) A specific brain tract guides follower growth cones in two regions of the zebrafish brain. J Neurobiol 23: 845–854

Coghill GE (1914) Correlated anatomical and physiological studies of the growth of the nervous system in amphibia. I. The afferent system of the trunk of *Amblystoma*. J Comp Neurol 24: 161–234

Coghill GE (1916) Correlated anatomical and physiological studies of the growth of the nervous system in amphibia. II. The afferent system of the head of *Amblystoma*. J Comp Neurol 26: 247–340

Covell DA, Noden DM (1989) Embryonic development of the chick primary trigeminal sensory-motor complex. J Comp Neurol 286: 488–503

Damas H (1944) Recherches sur le développement de *Lampetra fluviatilis* L. – contribution à l'étude de la cephalogénèse des vertébrés. Arch Biol Paris 55: 1–289

Dean B (1895) The early development of *Amia*. Quart J microsc Sci 38: 413–444

Easter SSJr, Ross LS, Frankfurter A (1993) Initial tract formation in the mouse brain. J Neurosci 13: 285–299

Eycleshymer AC, Wilson JM (1906) The gastrulation and embryo formation in *Amia calva*. Am J Anat 5: 132–162

Figdor MC, Stern CD (1993) Segmental organization of embryonic diencephalon. Nature 363: 630–634

Fraser EA (1915) The head cavities and development of the eye muscles in *Trichosurus vulpecula*, with notes on some other marsupials. Proc Zool Soc London 22: 299–346

Fraser S, Keynes R, Lumsden A (1990) Segmentation in the chick embryo hindbrain is defined by cell lineage restrictions. Nature 334: 431–435

Goette A (1914) Die Entwicklung der Kopfnerven bei Fischen und Amphibien. Arch mikr Anat 85: 1–165

Goodrich ES (1930) "Studies on the Structure and Development of Vertebrates" McMillan, London

Grande L, Bemis WE (1996) Interrelationships of Acipenseriformes, with comments on "Chondrostei." In "Interrelationships of Fishes" Ed by Stiassney MLJ, Parenti LR, Johnson GD, Academic Press, San Diego, pp 85–115

Hallerstein V (1934) Zerebrospinales Nervensystem (Kranialnerven). In "Handbuch der vergleichenden Anatomie der Wirbeltiere" Bd 2-1 Eds by Bolk L, Göppert E, Kallius E, Lubosch W, Berlin & Wien: Urban & Schwarzenberg.

Hartenstein V (1933) Early pattern of neuronal differentiation in the *Xenopus* embryonic brainstem and spinal cord. J Comp Neurol 328: 213–231

Holley J, Yu RK (1980) Localization of glycoconjugates recognized by the HNK-1 antibody in mouse and chick embryo during early neural development. Dev Neurosci 9: 105–119

Horigome N, Myojin M, Ueki T, Hirano S, Aizawa S, Kuratani S (1999) Development of cephalic neural crest cells in embryos of a cyclostome, *Lampetra japonica*, with special reference to the evolution of the jaw. Dev Biol 207: 287–308

Hughes A (1957) The development of the primary sensory system in *Xenopus laevis* (Daudin). J Anat 91: 323–338

Ishikawa Y, Zukeran C, Kuratani S, Tanaka S (1986) A staining procedure for nerve fibers in whole mount preparations of the medaka and chick embryos. Act Histochem Cytochem 19: 775–783

Jacob M, Jacob HJ, Wachtler F, Christ B (1984) Ontogeny of avian extrinsic ocular muscles. I. A light- and electron-microscopic study. Cell Tiss Res 237: 549–557

Jarvik E (1980) "Basic Structure and Evolution of Vertebrates" Vol 2, Academic Press, New York

Jefferies RPS (1986) "The Ancestry of the Vertebrates" British Museum (Natural History), London

Johnston MC (1966) A radioautographic study of the migration and fate of neural crest in the chick embryo. Anat Rec 156: 143–156

Keibel F (1906) Die Entwickelung der Äusseren Körperform der Wirbeltierembryonen, insbesondere der menschlichen Embryonen aus den ersten 2 Monaten. In "Handbuch der vergleichenden und experimentellen Entwickelungsgeschichte der Wirbeltiere" Ed by Hertwig O, 1ster Band, 2ter Teil, Gustav Fischer, Jena, pp 1–176

Kerr JG (1900) The external features in the development of *Lepidosiren paradoxa*. Phil Trans Roy Soc London Ser B 192: 299–330

Kerr JG (1901) The development of *Lepidosiren paradoxa*. Part II. Quart J microsc Sci 45: 1–40

Köntges G, Lumsden A (1996) Phombencephalic neural crest segmentation is preserved throughout craniofacial ontogeny. Development 122: 3229–3242

von Kupffer K (1891) The development of the cranial nerves of vertebrates. J Comp Neurol 1: 246–264, 315–332

von Kupffer K (1906) Die Morphologie des Centralnervensystems. In "Handbuch d. vergl. u. exp. Entwicklungslehre d. Wirbelthiere" Ed by Hertwig O, Bd. 2, 3ter Theil, Gustav Fischer, Jena, pp 1–272

Kuratani SC (1991) Alternate expression of the HNK-1 epitope in rhombomeres of the chick embryo. Dev Biol 144: 215–219

Kuratani S (1997) Spatial distribution of postotic crest cells defines the head/trunk interface of the vertebrate body: embryological interpretation of peripheral nerve morphology and evolution of the vertebrate head. Anat Embryol 195: 1–13

Kuratani SC, Bockman DE (1992) Inhibition of epibranchial placode-derived ganglia in the developing rat by bisdiamine. Anat Rec 233: 617–624

Kuratani SC, Hirano S (1990) Appearance of trigeminal ectopic ganglia within the surface ectoderm in the chick embryo. Arch Histol Cytol 53: 575–583

Kuratani S, Horigome N (2000) Developmental morphology of branhiomeric nerves in a cat shark, *Scyliorhinus torazame*, with special reference to rhombomeres, cephalic mesoderm, and distribution patterns of cephalic crest cells. Zool Sci (in press)

Kuratani S, Tanaka S (1990) Peripheral development of avian trigeminal nerves. Am J Anat 187: 65–80

Kuratani S, Ueki T, Aizawa S, Hirano S (1997) Peripheral development of the cranial nerves in a cyclostome, *Lampetra japonica*: morphological distribution of nerve branches and the vertebrate body plan. J Comp Neurol 384: 483–500

Kuratani S, Horigome N, Ueki T, Aizawa S, Hirano S (1998) Stereotyped axonal bundle formation and neuromeric patterns in embryos of a cyclostome, *Lampetra japonica*. J Comp Neurol 391: 99–114

Kuratani S, Horigome N, Hirano S (1999) Developmental morphology of the cephalic mesoderm and re-evaluation of segmental theories of the vertebrate head: evidence from embryos of an agnathan vertebrate, *Lampetra japonica*. Dev Biol 210: 381–400

Lamborghini JE, Revenaugh M, Spitzer NC (1979) Ultrastructural development of Rohon-Beard neurons: loss of intramitochondrial granules parallels loss of calcium action potentials. J Comp Neurol 183: 741–752

Landacre FL (1912) The epibranchial placodes in *Lepidosteus osseus* and their relation to the cerebral ganglia. J Comp Neurol 22: 1–69

Lumsden A, Keynes R (1989) Segmental patterns of neuronal development in the chick hindbrain. Nature 337: 424–428

Metcalfe WK, Myers PZ, Trevarrow B, Bass MB, Kimmel CB (1990) Primary neurons that express the L2/HNK-1 carbohydrate during early development in the zebrafish. Development 110: 491–504

Nieuwenhuys R (1997) Chondrostean fishes. In "The central nervous system of vertebrates" Vol 1, Ed by Nieuwenhuys R, Ten Donkelaar HJ, Nicholson C, Springer, Berlin, pp 701–757

Noden DM (1992) Spatial integration among cells forming the cranial peripheral nervous system. J Neurobiol 24: 248–261

Nordländer RH (1989) HNK-1 marks earliest axonal outgrowth in *Xenopus*. Dev Brain Res 50: 147–153

Nordländer RH (1993) Cellular and subcellular distribution of HNK-1 immunoreactivity in the neural tube of *Xenopus*. J Comp Neurol 335: 538–551

Northcutt RG (1993) A reassessment of Goodrich's model of cranial nerve phylogeny. Act Anat 148: 71–80

Northcutt RG, Brändle K (1995) Development of branchiomeric and lateral line nerves in the axolotl. J Comp Neurol 355: 427–454

Orr H (1887) Contribution to the embryology of the lizard. J Morphol 1: 311–372

Ostroumow A (1906) Zur Entwicklungsgeschichte des Sterletts (*Acipenser ruthenus*). II Die Myomeren des Kopfes. Zool Anz 30: 275–278

Platt JB (1891) A contribution to the morphology of the vertebrate head, based on a study of *Acanthias vulgaris*. J Morphol 5: 79–106

Romer AS, Parsons TS (1977) The Vertebrate Body. 5th Ed. Saunders, Philadelphia

Sadaghiani B, Vielkind JR (1990) Distribution and migration pathways of HNK-1-immunoreactive neural crest cells in teleost fish embryos. Development 110: 197–209

Schlosser G, Roth G (1995) Distribution of cranial and rostral pinal nerves in tadpoles of the frog *Discoglossus pictus* (Discoglossidae). J Morphol 226: 189–212

Schlosser G, Roth G (1997a) Evolution of nerve development in frogs. I. The development of the peripheral nervous system in *Discoglossus pictus* (Discoglossidae). Brain Behav Evol 50: 61–93

Schlosser G, Roth G (1997b) Evolution of nerve development in frogs. II. Modified development of the peripheral nervous system in the direct-developing frog *Eleutherodactylus coqui* (Leptodactylidae). Brain Behav Evol 50: 94–128

Sewertzoff AN (1911) Die Kiemenbogennerven der Fische. Anat Anz 38: 487–495

Spitzer NC, Baccaglini PI (1975) Changes in the ionic basis of the action potential in Rohon-Beard neurons during development. Soc Neurosci Abstr I, 1202 p 782

Spitzer NC, Baccaglini PI (1976) Development of the action potential in embryonic amphibian neurons *in vivo*. Brain Res 107: 610–616

Spitzer NC, Spitzer NC (1975) Time of origin of Rohon-Beard neurons in the spinal cord of *Xenopus laevis*. Am Zool 15: 781

Stone LS (1922) Experiments on the development of the cranial ganglia and the lateral line sense organs in *Amblystoma punctatum*. J exp Zool 35: 421–496

Tello JF (1923) Les différenciations neuronales dans l'embryon du poulet pendent les premiers jours de l'incubation. Trav Lab Invest Biol Univ Madrid 21: 1–93

Vaage S (1969) The segmentation of the primitive neural tube in chick embryos (*Gallus domesticus*). Adv Anat Embryol Cell Biol 41: 1–88

Vincent M, Duband JL, Thiery JP (1983) A cell surface determinant expressed early on migrating neural crest cells. Dev Brain Res 9: 235–238

Wedin B (1949) The development of the head cavities in *Alligator mississippiensis* Daud. Lunds Univ Arssikr NF avs 2 45: 1–32

Wedin B (1953a) The development of the head cavities in *Ardea*

cinerea L. Act Anat 17: 240–252
Wedin B (1953b) The development of the eye muscles in *Ardea cinerea* L. Act Anat 18: 38–48
Wilson SW, Ross LS, Parret T, Easter SS (1990) The development of a simple scaffold of axon tracts in the brain of the embryonic zebrafish, *Brachydanio rerio.* Development 108: 121–145
van Wijhe JW (1882) Über die Mesodermsegmente und die Entwicklung der Nerven des Selachierkopfes. Ver Akad Wiss Amsterdam, Groningen pp 1–50
Windle W (1970) Development of neural elements in human embryos of four to seven weeks gestation. Exp Neurol Suppl 5: 44–83
Windle WF, Austin MF (1936) Neurofibrillar development in the central nervous system of chick embryos up to 5 days of incubation. J Comp Neurol 63: 431–463

(Received February 24, 2000 / Accepted April 15, 2000)